# AXIAL COMPRESSION TEST OF THIN CIRCULAR CYLINDERS

A. LENGTH EFFECT

B. VISUAL STUDY OF BUCKLING

THESIS BY

Sunao Kanemitsu
Noble M. Nojima

In Partial Fulfillment of the Requirements for the Degree of Master of Science in Aeronautical Engineering.

California Institute of Technology
Pasadena, California
1939

TABLE OF CONTENTS

ACKNOWLEDGEMENT

We wish to thank Dr. E. E. Sechler and Dr. W. L. Howland for their guidance and generous aid in enabling us to present this thesis.

# DEFINITION OF SYMBOLS

| | |
|---|---|
| L | length |
| R | radius |
| t | thickness |
| E | Young's Modulus |
| P | compressive load |
| A | area $2\pi Rt$ |
| $\mu$ | Poisson's ratio |
| $\sigma$ | compressive stress |
| $\sigma_{Act.}$ | actual failure stress P/A |
| $\sigma_{crit.}$ | critical compressive stress |
| $\sigma_{theo}$ | refers to critical buckling failure stress $\frac{E}{\sqrt{3(1-\mu^2)}} \frac{t}{R}$ |

# SUMMARY

A.

This portion of the report contains results obtained from compression tests on 95 thin-walled steel circular cylinders. The tested cylinders were mainly of very small L/R ratio and large R/t ratio.

The results are compared with the existing theoretical failing stresses and are also presented in a non dimensional form, $\sigma/E$. The failure stress is best given by the equation $\sigma/E \simeq 9(t/R)^{1.6} + .16(t/L)^{1.3}$. This equation shall be limited for use for L/R greater than 0.1 and for L/R greater than 1.5 assume L/R = 1.5.

B.

A visual study of buckle formation is presented to aid future research which may be done on compression of thin cylinders.

# INTRODUCTION

In the summer of 1938 a careful study was ma de of all literatures pertaining to the strength of thin walled cylinders. One phase of this study lead to the obvious conclusion that there was very poor agreement between the theoretically predicted and the experimentally obtained failing load of such cylinders particularily for large R/t ratios. Also it was found that very little information was available on the effect of length on the strength properties of such thin unstiffened cylinders. As the size of airplanes has grown larger within recent years the R/t ratio of the fuselage has become larger without, however, an appreciable increase in the bulkhead spacing. It has been known that variation in length affect the strength properties of cylinders in compression and it is therefore very important to know definitely to what extent length influences the failure stress.

With these two problems in mind the research was conducted in two parts as following:

A. Testing of cylinders of various R/t ratio and with various lengths and especially cylinders whose lengths were shorter than the radius. Investigating cylinders in which the R/t ratios were higher than has been previously investigated.

B. A visual study of buckling of thin cylinders by deflecting the cylinders very slowly. Also, recording the wave pattern at different stages of deflection by measuring the sizes of buckles, and by photographing the specimens.

## HISTORICAL NOTES

The study of thin cylinders in compression is a very old problem. It was first studied experimentally by W. Fairbain in 1849. The first theoretical analysis of the problem was made by Lilly in 1906. A few years later, the theoretical studies were soon followed up by a number of authors among whom were Timoshenko (reference 1 page 439), Lorenz (reference 1 page 453), Southwell (reference 2), and Dean (reference 3). The theoretical analyses were based on cases where length effect was negligible.

The earliest theoretical analyses were based on symmetrical buckling, for which the critical stress became $\sigma_{CR} = \frac{E}{\sqrt{3(1-\mu^2)}} \frac{t}{R}$. The later theoretical analyses were based on the bending theory of thin shells as has been developed by Love. There are four solutions available:

1. Undefined type of buckling, axial wave length small.

   $$\sigma_{CR} = \frac{E}{\sqrt{3(1-\mu^2)}} \frac{t}{R}$$ same as symmetrical buckling case.

   It is often referred to as the Timoshenko or Lorenz form.

2. When only one half wave forms in the axial direction, that is when $\left(\frac{\pi R}{L}\right)^2 > \frac{2R}{t}\sqrt{3(1-\mu^2)}$ or another words length very short.

   $$\sigma_{CR} = \frac{\pi^2 E t^2}{12(1-\mu^2)L^2}$$ Euler's formula for elemental strip.

3. When cylinders are very long and break up as a strut without the formation of buckles.

   $$\sigma_{CR} = \frac{\pi^2 E R^2}{2L^2}$$ Euler's column.

4. When cylinders are of infinite length, and axial wave lengths are very large as compared with circumferential wave lengths.

$$\sigma_{CR} = 0.6 \frac{E}{\sqrt{3(1-\mu^2)}} \frac{t}{R}$$

Often refered to as Southwell's Case.

The accepted theoretical equation for critical stress is $\sigma_{CR} = \frac{E}{\sqrt{3(1-\mu^2)}} \frac{t}{R}$. The Southwell's case gives a lower value of stress but experiments have shown that axial wave lengths are equal to or less than the circumferential wave length. Failures of Southwell's type are not obtained practica lly.

Extensive experimental Investigation was started by Robertson (reference 4) in order to check the existing theoretical equation. Robertson was the one who pointed out the fact that failure of Southwell's type did not occur. He found that experimentally obtained stress was very low compared to the theoretical failing value. Wilson and Newmark (reference 5), interested in cylinders as a column, investigated the strength of thin cylinder, and likewise found the actual failing stresses very low.

With an introduction of the stressed skin type of airplane construction, there was renewed interest in the instability problem of thin shells. Sanden and Tölke (reference 6), and Flugge(reference 7), made theoretical analyses, however, they have arrived at a similar result as that obtained by earlier investigators. Recently Donnell (reference 8), has advanced a new large deflection theory considering initial deformation. Donnell believes that the lowness of the experimental failing stress was due to the fact that it is practically impossible to make a mathematically correct cylinder under ordinary circumstances.

There has also been intensive experimental investigation in recent years. At the N.A.C.A., Lundquist (reference 9), has made tests on Dural, in which he compares the results with the theory and gives an equation for failure. Donnell has made tests at GALCIT on steel and brass in an attempt to check the classical theory and Flugge has run tests on celluloid cylinders. However, none of these experiments reached a higher value than 60% of the theoretical va lue.

Wagner and Ballersted (reference 10) have done experimental work on cylinders to find the length effect. They ran tests on brass cylinders for which the L/R va lues were as low as .50 and the R/t values as high as 4000, and have given an emperical design formula, $\frac{\sigma}{E} = .2\frac{t}{R} + 3.3\left(\frac{t}{L}\right)^2$.

# PART A

# LENGTH EFFECT OF THIN-CIRCULAR CYLINDERS IN AXIAL COMPRESSION

## EQUIPMENT AND TEST PROCEDURE

The material used for these tests was standard shim stock steel. The tests were conducted on six different thicknesses, the nominal thickness varying from .002" to .009". With these thickness the test cylinders had a R/t range from 750 to 3000, since the fabricated cylinders had a radius of 6.375". The thicknesses of the material were measured with an ordinary micrometer of least reading 1/1000 inch and measurements were approximated to 1/10 of this value.

The mechanical properties of these shim stock varied for every thickness and it was necessary to find the Young's Modulus for each thickness (table 1). The stress strain relation was obtained for the material in tension in the direction in which the material was to be compressed as a finished cylinder. The work was done in a Riehle 3000# testing machine (see figure 1). The strain for the material was measured with an Ame's dial in a specially balanced frame. The strain gage read directly in 1/10,000 unit strain and could consistently be read to 1/10 of this value.

The cylinder was attached to bulkhead shown in figure 2, of special design with built in clamps. These clamps were 1/2 inch deep, and each clamp was tightened with a single screw. These bulkheads made the cylinder fabrication simple and fast, since no jig was required.

In fabricating the cylinder, the shim stock was cut to the length of the developed surface and placed in the bulkhead. To control the height of the cylinder, the edge

which went between the clamps was milled so that the edges were parallel and straight. This is very important for this method. The seam was closed by soldering a 1/2 inch wide strap over the joint. The soldering process is very important because any thermal expansion of the sheet during the process of soldering usually left a buckle or a soft spot in the cylinder wall. Figure 3 shows a soldered specimen ready to be tested.

Figure 4 shows the test apparatus with the specimen in position. The load is applied by the jack and transmitted through the ring which measures the load to the test cylinder. The ball universal joint between the ring and the cylinder bulkhead transmits load only in the vertical direction. The ball cup is centered on the centering pin built in the bulkhead. The test cylinder was leveled and the calibra ted ring was aligned vertically so that dial deflection reading was in the vertical direction. Load was applied slowly but continuously and only failure loads were noted. Specimens of very short length which took very large loads were tested in a 15000# standard testing machine.

## FAILURE OF SHORT SPECIMENS

In figure 5 is shown a failure picture of specimen of very short length. Investigation has shown that it is a failure of Euler elemental strip with fixed end. This type of failure occurred for specimen which L/R was less than about .12 for R/t of 750. For R/t = 3000 the L/R ratio was less the .07. Such failure occurred with a sudden collapse on steady rise in load.

Figure 6 shows a failure of the cylinder with twisting. Such failure occurred for specimen up to L/R ra tio of .3 for thicker material and smaller L/R for thinner material. This failure is a very interesting failure.

It is believed that as soon as the buckles form, the edges in the axial direction of the buckles are unstable and thus go into the form of least resistance. In this case the resistance of these edges in the circumferential direction is the lowest and thus the cylinder twists. For specimens with L/R value from .20 to .25 the twist was found to be about .0063 radians.

## DISCUSSION OF RESULTS

The experimental data were reduced in form of $\sigma_{ACT} = \frac{P}{A}$ The corresponding theoretical critical stress calculation were made using $\sigma_{THEO} = \frac{E}{\sqrt{3(1-\mu^2)}} \frac{t}{R}$. These stresses were put in the ratio of $\sigma_{ACT}/\sigma_{THEO}$ to get a dimensionless number. Also the data were reduced to another form of dimensionless number $\frac{\sigma}{E}$ as was used by Lundquist. Experimental Data of Donnell, Lundquist, and Wilson and Newmark were taken from N.A.C.A. TR. 473. Lundquist has the values in form of $\sigma/E$ , which were changed over to $\sigma_{ACT}/\sigma_{THEO}$ . Wagner's test data on Brass were also reduced to form of $\sigma_{ACT}/\sigma_{THEO}$ . The published data of Wagner's tests do not include the value of Elastic Modulus of his material. The value of E for his tests was assumed to be $16.0 \times 10^6 \#/in^2$.

With an assumption of "no length effect", the $\sigma_{ACT}/\sigma_{THEO}$ of all tests are plotted against R/t in figure 7. The present tests have extended considerably the range of investigated R/t, but also have increased the scatter of points. A recommended design formula which some designers have been using for dural is $\sigma_{CR} = .605\, E \left(\frac{t}{R}\right)^{1/6}$. This is written in form $\frac{\sigma_{ACT}}{\sigma_{THEO}} = \left(\frac{t}{R}\right)^{1/6}$ and plotted as a dotted line.

The ratio $\sigma_{ACT}/\sigma_{THEO}$ for the data obtained by the authors was next plotted against L/R for a constant R/t ratio in Figure 8 to Figures 13. In these plots it was found that certain variations of R/t were permissable and still have the points stay within the range of experimental scatter. For R/t of 750, such allowable variation was between 700 and

800. For R/t of 3000, the allowable variation increased to a limit between 2600 to 3400. A curve was drawn through these points and finally combined on a single graph of $\sigma_{ACT}/\sigma_{THEO}$ plotted against L/R for a constant R/t as in Figure 15. A cross plot was made from figure 15 to get a curve of $\sigma_{ACT}/\sigma_{THEO}$ versus R/t for a constant L/R as in figur e 16. In order to plot such a family of smooth curves as in figure 15 and 16, each individual curve in figure 8 to figure 13 was varied to make up a smooth family satisfying the experimental data.

The Euler equation for the buckling stress of an elemental strip is $\sigma_{CR} = \frac{\pi^2 E t^2}{3(1-\mu^2)L^2}$ for fixed end. Noting that for very short lengths, the failure was of this type, this equation was put in the form of $\sigma_{CR}/\sigma_{THEO}$, where $\sigma_{THEO}$ is the critical stress for buckling;

$$\frac{\sigma_{CR}}{\sigma_{THEO}} = \frac{\pi^2}{\sqrt{3(1-\mu^2)}} \frac{tR}{L^2} \quad \text{OR} \quad \frac{\pi^2}{\sqrt{3(1-\mu^2)}} \frac{t}{R}\left(\frac{R}{L}\right)^2$$

This curve was expected to follow the experimental curve in regions where the L/R ratio was less than .05 from R/t ratios of 2000, and 3000, experimental curve approaches the Euler but the experimental are somewhat too low.

From the published data of the experimental work of Donnell, Lundquist, Wilson and Newmark, and Wagner and Ballerstedt, the data which were within our experimental range of L/R and with R/t's that are within the allowable R/t variation were spotted on the curves. Lundquist's and Wagner's data give points which are equal to or higher than those obtained by the authors but are still within the range of the experimental scatter.

Donnell's test data are for L/R = 2 and fits the extended curves well. Wilson and Newmarks tests give consistantly lower values. The curves for R/t = 1000 and 1600 have been extended to L/R values beyond the investigated points on the strength of these published data.

In figure 14 the curve for R/t = 500 was drawn from the experimental data given by Wagner. Because it seems to fit the family of curves on figure 15 very well, the curve was extended to lower L/R values and other published da ta were spotted in. This curve was not used in cross plotting for $\frac{\sigma_{ACT}}{\sigma_{THEO}}$ versus R/t.

The cylinders investigated by Lundquist were made of dural and had a radius of 7.5 inches and 15". Wagner's cylinders were made of brass with radius of 4 and 8 inches, but as previously mentioned, the Elastic Modulus is unknown. Donnells tested cylinders of brass and steel for which exact dimensions are unknown, however, they are cylinders of very small radius. Wilson and Newmark tested cylinders of steel in which the radius varied from 2 to 40 inches. High value given by Lundquist and Wagner may be due to the large cylinders although the Wilson and Newmark tests do not indicate that such would be expected.

As mentioned earlier, there are 3 solutions obtainable from the thin shell bending theory. They are

$$\sigma_{CR} = \frac{\pi^2 E t^2}{12(1-\mu^2)L^2}$$ Euler elemental strip

$$\sigma_{CR} = \frac{E}{\sqrt{3(1-\mu^2)}} \frac{t}{R}$$ Buckling range

$$\sigma_{CR} = \frac{\pi^2 E R^2}{2L^2}$$ Euler column

In figure 17 and 18 these 3 different critical ranges are plotted in form of $\frac{\sigma_{CR}}{\sigma_{THEO}}$ versus L/R. The Euler elemental strip equation was multiplied by 4 to satisfy the end fixity condition. Also the Euler column formula wa s multiplied by 4 to give a condition of fixed end. Theoretically, with these 3 formulas the critical stresses for all lengths of cylinders should be predictable. In figure 17 and 18 it should be noted that scale of L/R at 1.0 is discontinuous and jumps to 100. $\frac{\sigma_{CR}}{\sigma_{THEO}}$ for buckling and experimental are constant through range of 10. The experimental curve also has been drawn together with theoretical curves for the 3 regimes of failure. The experimental curve only approaches the theoretical at very small and very large L/R values, both cases being out of the buckling range. At very large L/R values Southwell's case must hold but there is no way of designating such points.

## POSSIBLE DESIGN APPLICATION

Wagner has developed an empirical design formula

$$\sigma_E = .2\left(\frac{t}{R}\right) + 3.3\left(\frac{t}{L}\right)^2$$

This formula fits the experimental points very well for an R/t value of 750 except that the stresses given by the formula are too low between L/R of 0.2 and 0.5. For large R/t values the formula gives stresses which are too high for L/R values greater than 0.4.

A new design empirical formula has been developed by the authors on the basis of all of the experimental information available, this formula having the sa me form as that of Wagner. The same variables are used $\left(\frac{t}{R}\right)$ and $(t/L)$ or $\left(\frac{t}{R}\frac{R}{L}\right)$, but the constant coefficients and the exponent s have been altered. The authors' formula is

$$\sigma_E = 9\left(\frac{t}{R}\right)^{1.6} + .16\left(\frac{t}{L}\right)^{1.3}$$

The experimental values reduced to the form $\sigma_E$ has been plotted against L/R for constant R/t in figures 19 and 20. The emperical design formula is calculated for a given R/t and drawn through the points as a curve. Between L/R of 0.1 and 1.5 all curves seem to fit the points fairly well. For L/R values greater than 1.5, the L/R ratio can be assumed to equal 1.5 since the tests have shown that there is no consistent decrease in stress due to increase above 1.5. This can be best seen by analyzing Donnell's test results in which he has investigated L/R ratio from 2.0 to as high as 32.

The question arises with such design formula whether it can be applied safely to other materials. In figures 8 to 14 data on brass and dural are plotted. Although these data give consistantly a somewhat higher critical stress,

the points are well within the range of experimental scatter of the data for which the formula was derived.

# PART B

## Visual Study of the Buckling Process of Thin Circular Cylinders

PART B

## THE BUCKLING WAVE PATTERN OF THIN CYLINDERS UNDER COMPRESSION

The great discrepency between the theoretically predicted and experimentally obtained failing loads of thin walled cylinders would lead to the conclusion that some of the assumptions made in the theoretical treatment of the problem were not valid. One of the basic assumptions made by all of the investigators was regarding the form of the buckling wave pattern. For this reason the authors endeavored to slow up the buckling phenomenon so that the development of the buckles would be studied and the sizes of the initial waves measured.

In order to cause buckling to take place slowly it was necessary to add the load to the cylinder head with some form of jack and applying external load enough to fail the specimen, the load being varied by the jacks. The head was then lowered by small increments and the development of the wave pattern was started.

## APPARATUS AND TEST PROCEDURE

Since the cylinders were made by means of a heavy plate head and base the supporting jack was placed within the cylinder (See fig. 21). The jack consisted of 3 set screws which held the head of the cylinder and rested on a $\frac{3}{4}$ inch plate. These set screws afforded adjustment of the cylinder head. The $\frac{3}{4}$ inch plate was either lowered or raised by means of three $\frac{1}{2}$ inch diameter screws which rested on the base of the cylinder, these $\frac{1}{2}$ inch screws being rotated by means of a gear system. Five inch gears were placed on the $\frac{1}{2}$ inch screws while a two inch gear was in the center and was used as the driver. (See fig. 22). The small gear was attached to a shaft which extended through the base of the cylinder and could be turned externally by a wrench. The $\frac{1}{2}$ inch screws were threaded with S.A.E. N.F. series and had twenty threads to the inch. The gear ratio was 2 to 5 and thus by turning the driver gear slightly a very small relative movement between the heads could be obtained.

Since loads required to fail the cylinders were not over 3000 pounds, a simple loading device was set up in order that photographs could more easily be

obtained. This device (See fig 23) merely consisted of two supporting members and a cross bar. At the center of the cross bar a loading screw was placed. The specimen lay on two supporting bars in order to allow a wrench to get underneath the specimen to turn the gears. The specimen was connected to the loading screw by means of ball points with a calibrated ring in between to measure the load.

The specimens used were of the same type as those discussed in the first part of this report. They were made of the same shim stock and in exactly the same manner. After the specimen was made, it was placed under the loading device and then aligned in order to have the load vertical. Two dial gauges were placed on the specimen in such a way as to obtain the deflection. After the set screws were adjusted, a load was applied which was beyond the failing load of the specimen determined from previous tests. The head of the cylinder was slowly lowered and when buckles appeared observations were taken. The size and location of the buckle and deflection of the specimen were measured for every picture taken. Upon further lowering of the head, the buckles would move or increase in size and at each appreciable change further data were taken. Only buckles which appeared on the side facing the camera were measured. This seemed sufficient as a good average could be obtained from one side.

Under this set up the thicker specimen would not show a movement of the buckles but only a sudden wrinkle pattern at failure. In some cases a few scattered wrinkles would appear and move slightly, but even with very slow lowering of the head the failure pattern would suddenly occur and details of its formation could not be obtained. Figures 24 and 26 represent one of the thicker specimen with an R/t of 1250 and L/R of 1.41. Thus only the one thin specimen with a thickness of .0034 inches was photographed.

# DESCRIPTION AND COMMENTS OF BUCKLING PROCESS

## Specimen P-18

L - 9 in. L/R - 1.41 Material - Steel

t - .0034 in. R/t - 1875

## Figure 27

No Load

## Figure 28

Deflection N - 0 mm. S - .01 mm. Av. - .005 mm.

| Buckle No. | Length Circum. in. | Height Axial in. | Dist. From Bottom in. | Axis Angle with Horizontal Deg. | Position From right |
|---|---|---|---|---|---|
| A | 1 1/8 | 1 | 2 | 45 | 2 |
| B | 1 3/4 | 1 1/4 | 2 | 0 | 1 |
| C | 1 | 3/4 | 3/4 | 0 | 3 |

These were the first buckles to form and they appeared simultaneously. Buckle A had an elliptical shape whose axis was at an angle. Buckle C was probably due to thinness of the sheet at that point. These two buckles do not seem to form any definite pattern.

Specimen P-18 continued

Figure 29

Deflection N - 0 mm. S - .02 mm. Av. - .01 mm.

| Buckle No. | Length Circum. in. | Height Axial in. | Dist. From Bottom in. | Axis Angle with Horizontal Deg. | Position from right |
|---|---|---|---|---|---|
| A | 2 | 1 1/2 | 3 | 45 | 3 |
| B | 1 3/4 | 1 1/8 | 2 1/2 | -30 | 1 |
| C | 1 | 7/8 | 3/4 | 0 | 2 |
| D | 1 1/4 | 1 1/8 | 6 | 0 | 2 |
| E | 1 1/2 | 7/8 | 3 1/2 | 45 | 4 |

New buckles formed with the existing ones becoming larger. Buckle B, with the increase in size, started to rotate its axis in conforming with the pattern which was forming on the right side of the specimen. Notice should be taken of Buckle D which has formed near the top. Buckle C has hardly changed and can be considered as local buckling due to imperfection of the sheet. All the new buckles were of elliptical shape some of whose axis were at an angle.

Figure 30

Deflection N - 0 mm. S - .053 mm. Av. - .0265

| Buckle No. | Length Circum. in. | Height Axial in. | Dist. From Bottom in. | Axis Angle with Horizontal Deg. | Position from Right |
|---|---|---|---|---|---|
| A | 2 | 1 1/2 | 3 | 0 | 3 |
| B | 2 3/8 | 1 1/4 | 2 1/2 | -45 | 1 |
| C | Has become smaller | | | | |
| D | 1 7/8 | 1 1/2 | 5 | 0 | 2 |
| E | 2 | 1 3/8 | 5 | 30 | 4 |
| F | 1 3/4 | 1 1/8 | 1 1/4 - 4 | 30 | 5 |

A group of four new buckles (F) have formed to the left

Specimen P-18 (continued)

whose size are practically equal. All their axes are at an angle and are forming a definite pattern. All the originals have increased in size with the exception of C. Buckle D has dropped and Buckle E moved to the right in forming a pattern with A and B. The axes of both A and B have rotated.

Figure 31

Deflection N - .015 mm. S - .143 mm. Av. - .129 mm.

| Buckle No. | Length Circum. in. | Height Axial in. | Dist. From Bottom in. | Axis Angle with Horizontal Deg. | Position From Right |
|---|---|---|---|---|---|
| A | 2 3/8 | 1 1/2 | 3 1/2 | 30 | 3 |
| B | 2 1/8 | 2 | 4 | 0 | 1 |
| C | Still very small | | | | |
| D | 2 1/2 | 2 | 5 | 0 | 2 |
| E | 2 1/2 | 2 1/2 | 5 | 15 | 4 |
| $F_1$ | 2 | 1 1/4 | 4 | 45 | 6 |
| $F_{2,3,4}$ | 2 3/8 | 1 3/8 | 1 - 5 | 30 | 5 |

The last formed group of Buckles (F) have increased in size forming a continuation with the pattern of the other group. This group has shifted to the left with $F_1$, the one on extreme left, nearly out of the picture. Buckle A has rotated its axis while B has moved more to the right connecting with the pattern on the side of the cylinder.

Specimen p-18 continued

Figure 32

Deflection N - .105 mm. S - .403 mm. Av. - .254 mm.

| Buckle No. | Length Circum in. | Height Axial in. | Dist. From Axis Bottom in. | Angle with Horizontal Deg. | Position From Right |
|---|---|---|---|---|---|
| A. | 2 3/4 | 2 3/8 | 3.5 | 0 | (2) |
| B | Shifted into one coming from right | | | | |
| C | Still no change | | | | |
| D | 3 | 3 | 5 | 0 | (1) |
| E | 2 7/8 | 2 1/2 | 5 | 0 | (3) |
| F 1 | Shifted out of picture to left | | | | |
| F 2 | 3 1/4 | 3 | 3 | 0 | (4) |
| F 3 | 3 | 2 5/8 | 5 | 0 | (5) |
| F 4 | 2 3/8 | 2 1/4 | 2 1/2 | 0 | (6) |

This picture shows the whole side in failure. The F group has now become as large as the original and there is formed the final pattern. The buckles are of diamond shape with sides of equal length. The axes of all the large buckles are nearly horizontal. There are now several small buckles forming on the top and bottom similar to buckle C.

## Comments on Specimen P-18

In the specimen of which the picture was taken the failure first occurred at the right. Thus the deflections were not symmetrical. Likewise buckles formed first on the right and new ones formed to the left as the load increased.

It can be seen from the dimensions of the wrinkles that at first they were of elliptical shape with the major axis at some angle. As more load was applied there was a continual change till a failure pattern of square or diamond shaped buckles with horizontal axis was formed.

Many other samples of the same thickness and length were slowly failed and observed. The final failure form seemed to be the large diamond shape inner pattern with small buckles along the edge. In most cases a single buckle was formed first due to, perhaps, some irregularity in the material. Then as more load was applied buckles formed around the original one of about the same size. They gradually

went into the final failure pattern as load was applied. The new buckles generally started either below or above this group and then worked up or down as the case may be until they merged into the final pattern. In many cases small buckles formed which shifted or were absorbed into the previously formed larger ones.

## Specimen P-19

P - 19 t - .0034 L - 6 Material - Steel
R/t - 1870 L/R - .94

### Figure 33

No Load

### Figure 34

Deflection N - .013 mm. S - .015 mm. Av. - .014 mm.

| Buckle No. | Length Circum in. | Height Axial in. | Dist. From Bottom in. | Axis Angle with Horizontal Deg. | Position From Right |
|---|---|---|---|---|---|
| A | 2 | 1 | 2 1/4 | 45 | 5 |
| B | 1 7/8 | 1 3/8 | 2 3/4 | 0 | 4 |
| C | 2 | 1 1/4 | 2 1/4 | 45 | 3 |
| D | 1 7/8 | 1 1/4 | 2 3/4 | 0 | 2 |
| E | 1 3/4 | 1 1/4 | 2 1/4 | 45 | 1 |
| F | 3/4 | 3/4 | 3/4 | 0 | 6 |

All the buckles appeared at the same time. The angle of the axes alternated with adjoining buckles. The sizes were very nearly the same and they were elliptical in shape. It can be seen that the general failure pattern was formed from the beginning. Buckle F on the far lower left side was similar to Buckle C of the first specimen.

### Figure 35

Deflection N - .028 mm. S - .033 mm. Av. - .0305 mm.

| Buckle No. | Length Circum. in. | Height Axial in. | Dist. From Bottom in. | Axis Angle with Horizontal Deg. | Position From Right |
|---|---|---|---|---|---|
| A | 1 3/4 | 1 1/4 | 1 7/8 | 0 | 5 |
| B | 2 | 1 3/4 | 2 1/8 | 30 | 4 |
| C | 2 1/8 | 1 3/4 | 2 3/8 | 0 | 3 |
| D | 2 3/8 | 1 3/8 | 2 3/4 | 45 | 2 |
| E | 2 1/4 | 1 3/4 | 2 1/2 | -45 | 1 |
| F | 1 | 1 | 3/4 | 0 | 6 |

The original buckles have increased in size and rotated

Specimen P-19 continued

their axes. There are many new buckles forming between the originals of the size 1 by 1. These are making up the links for the final form and are mainly above with a few below the originals.

Figure 36

Deflection N - .057 mm. S - .076 mm. Av. - .0665 mm.

| Buckle No. | Length Circum. in. | Height Axial in. | Dist. From Bottom in. | Axis Angle with Horizontal Deg. | Position From Right |
|---|---|---|---|---|---|
| A | 1 3/4 | 1 3/8 | 2 1/4 | 30 | 5 |
| B | 1 3/4 | 1 7/8 | 2 1/2 | 0 | 4 |
| C | 2 1/4 | 1 3/4 | 2 1/4 | -30 | 3 |
| D | 2 7/8 | 1 1/2 | 2 1/2 | 45 | 2 |
| E | 2 1/2 | 1 1/2 | 2 1/2 | 45 | 1 |
| F | Become small | | | | |

The main change in this picture is the increase in size of the last appearing buckles to about 1 3/4 by 1 3/4. The lower ones did not show much of an increase in size. The axes of the original buckles made noticeable rotations.

Figure 37

Deflection N - .105mm. S - .13 mm. Av. - .1175 mm.

| Buckle No. | Length Circum. in. | Height Axial in. | Dist. From Bottom in. | Axis Angle with Horizontal Deg. | Position From Right |
|---|---|---|---|---|---|
| A | 2 1/4 | 1 1/2 | 2 1/4 | 0 | 5 |
| B | 2 1/4 | 2 1/4 | 2 1/4 | 0 | 4 |
| C | 2 1/4 | 2 1/4 | 2 1/4 | 0 | 3 |
| D | 2 1/2 | 2 1/4 | 2 1/2 | 30 | 2 |
| E | 2 1/2 | 2 1/2 | 2 1/2 | -30 | 1 |
| F | Still small | | | | |

Many new buckles were formed near the edges of the cylinder

Specimen P-19 continued

of about the size 1 by 1. The buckles which appeared in picture 35 above the originals have now the size of 2 1/4 by 2 1/4. Thus they are now of the same size and completing the failure pattern with the originals. Notice that all the larger buckles are of the same size and that the axes are nearly all horizontal.

Figure 38

Deflection N - .16 mm. S - .212 mm. Av. - .186 mm.

All the original buckles remained the same size with D and E becoming slightly smaller and rotating their axes to the horizontal position. The buckles in the top row have now formed the failure pattern with the originals. The smaller buckles which were below the originals have now been absorbed by them. There are till the smaller buckles along the edges of the cylinder.

## Comments on Specimen P-19

On this specimen single buckles did not form at first but a pattern of a whole group formed simultaneously with new ones forming as the load increased. The same phenomenon occurred as that noted previously, that is, the waves were first elliptical and then went into a diamond or square shape. The final failure pattern was very similar to that obtained in the longer specimen.

Many cylinders of the same dimensions were failed and the wrinkle formation was similar but in the other cases, the failure pattern occurred much more rapidly and the change could not be observed as well as is shown in the photographs.

## Specimen P-20

L - 3 L/R - .47 Material - Steel
t - .0034 R/t - 1870

### Figure 39

No Load

### Figure 40

Deflection N - 0 mm. S - .018 mm. Av. - .009 mm.

| Buckle No. | Length Circum. in. | Height Axial in. | Dist. From Bottom in. | Axis Angle with Horizontal Deg. | Position From Right |
|---|---|---|---|---|---|
| a | 1 1/4 | 3/4 | 1/2 | 0 | 1 |
| b | 1 | 1/2 | 1/2 | 0 | 2 |

The two buckles seen in this picture are probably due to local imperfections and did not seem to effect the final failure pattern. However, the occurrence of the failure pattern was so fast that it could not be observed if buckles a and b had any effect.

## Specimen P-20 continued

### Figure 41

| Buckle No. | Length Circum. in. | Height Axial in. | Dist. From Bottom in. | Axis Angle with Horizontal Deg. | Position From Right |
|---|---|---|---|---|---|
| A | 1 1/8 | 1 1/4 | 1 1/4 | 0 | 1 |
| B | 1 1/4 | 1 | 1 1/4 | 0 | 3 |
| C | 1 | 3/4 | 1 1/4 | 0 | 5 |
| D | 1 | 3/4 | 1 1/4 | 0 | 7 |
| E | 1 1/4 | 3/4 | 3/4 | 0 | 2 |
| F | 1 1/2 | 1 | 3/4 | 0 | 4 |
| H | 1 1/4 | 7/8 | 3/4 | 0 | 6 |
| I | 1 | 3/4 | 3/4 | 0 | 8 |

### No Picture

Deflection N - .01 mm. S - .10 mm. Av. - . 055 mm.

| Buckle No. | Length Circum. in. | Height Axial in. | Dist. From Bottom in. | Axis Angle with Horizontal Deg. | Position From Right |
|---|---|---|---|---|---|
| A | 1 3/4 | 1 1/4 | 1 3/4 | 0 | 1 |
| B | 1 1/2 | 1 1/4 | 1 3/4 | 0 | 3 |
| C | 1 1/2 | 1 | 1 1/2 | 0 | 5 |
| D | 1 1/2 | 1 1/4 | 1 1/2 | 0 | 7 |
| E | 1 3/4 | 1 | 1/2 | 0 | 2 |
| F | 1 1/4 | 1 | 1/2 | 0 | 4 |
| H | 1 1/2 | 1 | 3/4 | 0 | 6 |
| I | 1 | 3/4 | 3/4 | 0 | 8 |

No picture was taken as the only change was slight increase in size of the buckles.

## Comments on Specimen P-20

In this case the buckles all formed simultaneously in the final failure pattern. This was also observed in the failure of other specimen of the same type. As more load was applied the movement of the buckles was slight and only an increase in size was noticed. The buckles in this case were from the beginning not of elliptical shape but of the diamond or square shape. No appreciable movement or growth of the failure pattern could be observed in these shorter specimen.

## GENERAL DISCUSSION OF RESULTS

It should be noted that the shim stock used had irregularities and perhaps was the cause of singular buckles forming and disappearing.

In the final failure of all the specimens the buckles had the same pattern and shape. However the size varied slightly with the length of the specimen. Even though the radius was the same in every case, the circumferential size of the buckles was not the same at failure but varied with the length of the cylinder, that is, the longer cylinders had buckles with the longest circumferential length.

It can be concluded that in thin long cylinders there is a definite movement of the buckles from its original position to final failure. However, in shorter or thicker specimen the failure pattern appeared to be formed almost instantaneously with little movement of buckles. However, with more refined test apparatus it might be possible to slow down the process still further so as to obtain a gradual development of the wave form in the shorter specimens. This

should probably be done in any future research on the problem.

The results obtained so far indicate that the initial buckled state of the cylinder is quite different from that assumed for previous theoretical work in the problem. It is hoped that this information will be of assistance in guiding future theoretical treatment so that a more accurate prediction of the critical failing stress of such cylinders can be obtained.

Table 1

| nominal thickness | Young's Modulus |
|---|---|
| .002 in. | 33.5 x $10^6$ #/in. |
| .003 | 32.0 x $10^6$ |
| .004 | 32.4 x $10^6$ |
| .005 | 31.5 x $10^6$ |
| .006 | 30.6 x $10^6$ |
| .0085 | 29.0 x $10^6$ |

Variations of Young's Modulus with thickness

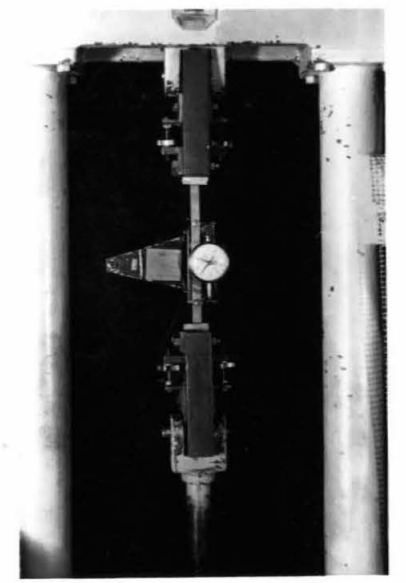

Fig.1
Tension Test Apparatus
in Reihle Testing Machine.

Fig.2
Cylinder Bulkhead

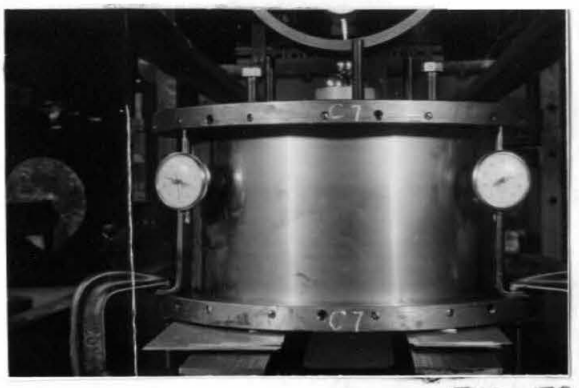

FIG. ~~53~~ 49

Fig.3
Assembled Cylinder

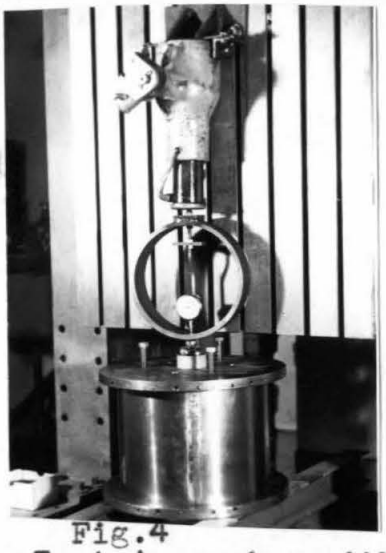

FIG. 48

Fig.4
Test Apparatus with
Specimen in Position.

Fig.5
Failure of Euler
Elemental Strip

Fig.6
Failure with Torsion

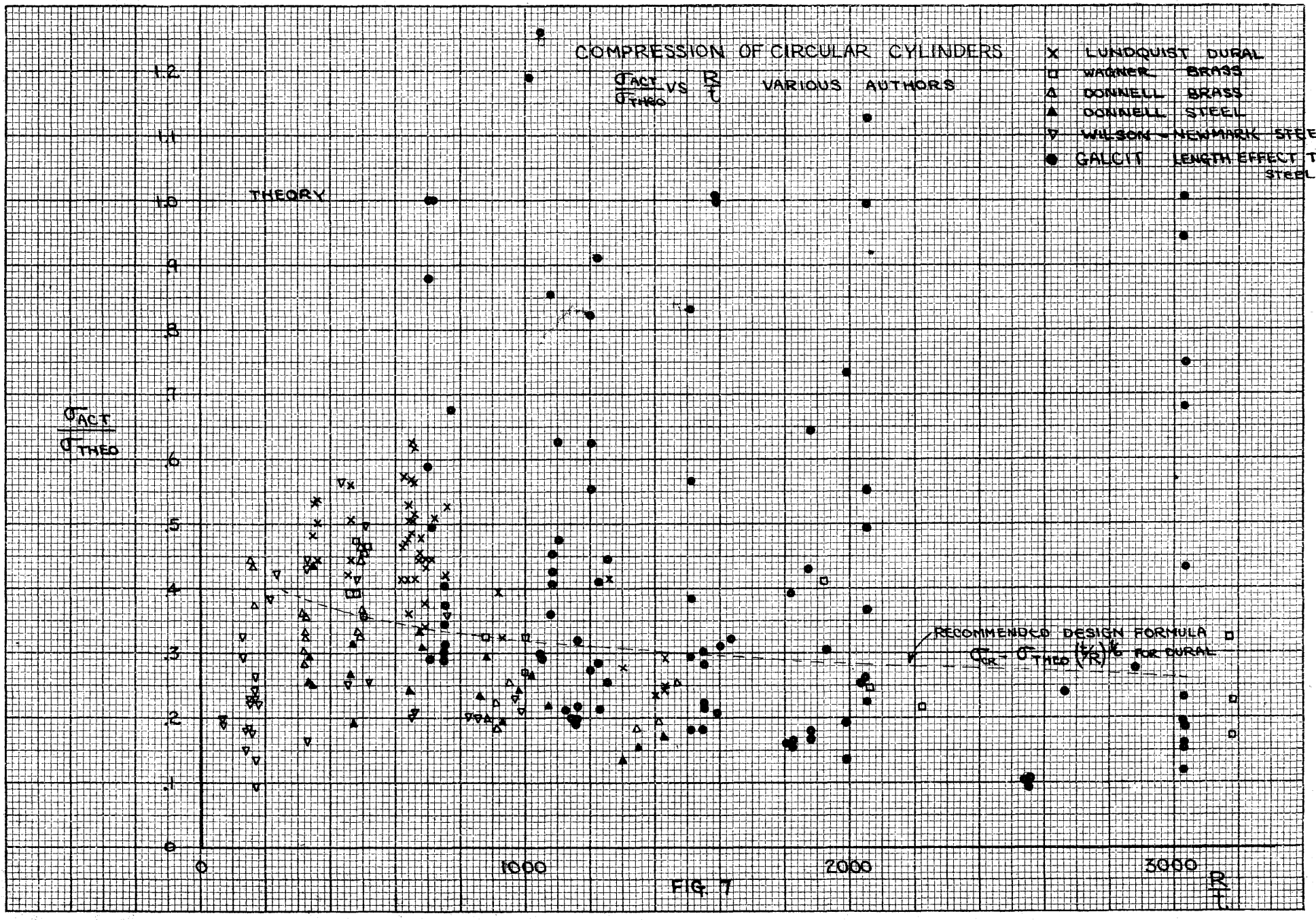
COMPRESSION OF CIRCULAR CYLINDERS
$\frac{\sigma_{ACT}}{\sigma_{THEO}}$ VS $\frac{R}{t}$ VARIOUS AUTHORS
X LUNDQUIST DURAL
□ WAGNER BRASS
△ DONNELL BRASS
▲ DONNELL STEEL
▽ WILSON - NEWMARK STEEL
● CALCIT LENGTH EFFECT TEST STEEL
THEORY
$\frac{\sigma_{ACT}}{\sigma_{THEO}}$
RECOMMENDED DESIGN FORMULA
$\sigma_{CR} = \sigma_{THEO}\left(\frac{t}{R}\right)^{\frac{1}{3}}$ FOR DURAL
1.2
1.1
1.0
.9
.8
.7
.6
.5
.4
.3
.2
.1
0
0
1000
2000
3000
$\frac{R}{t}$

FIG. 7

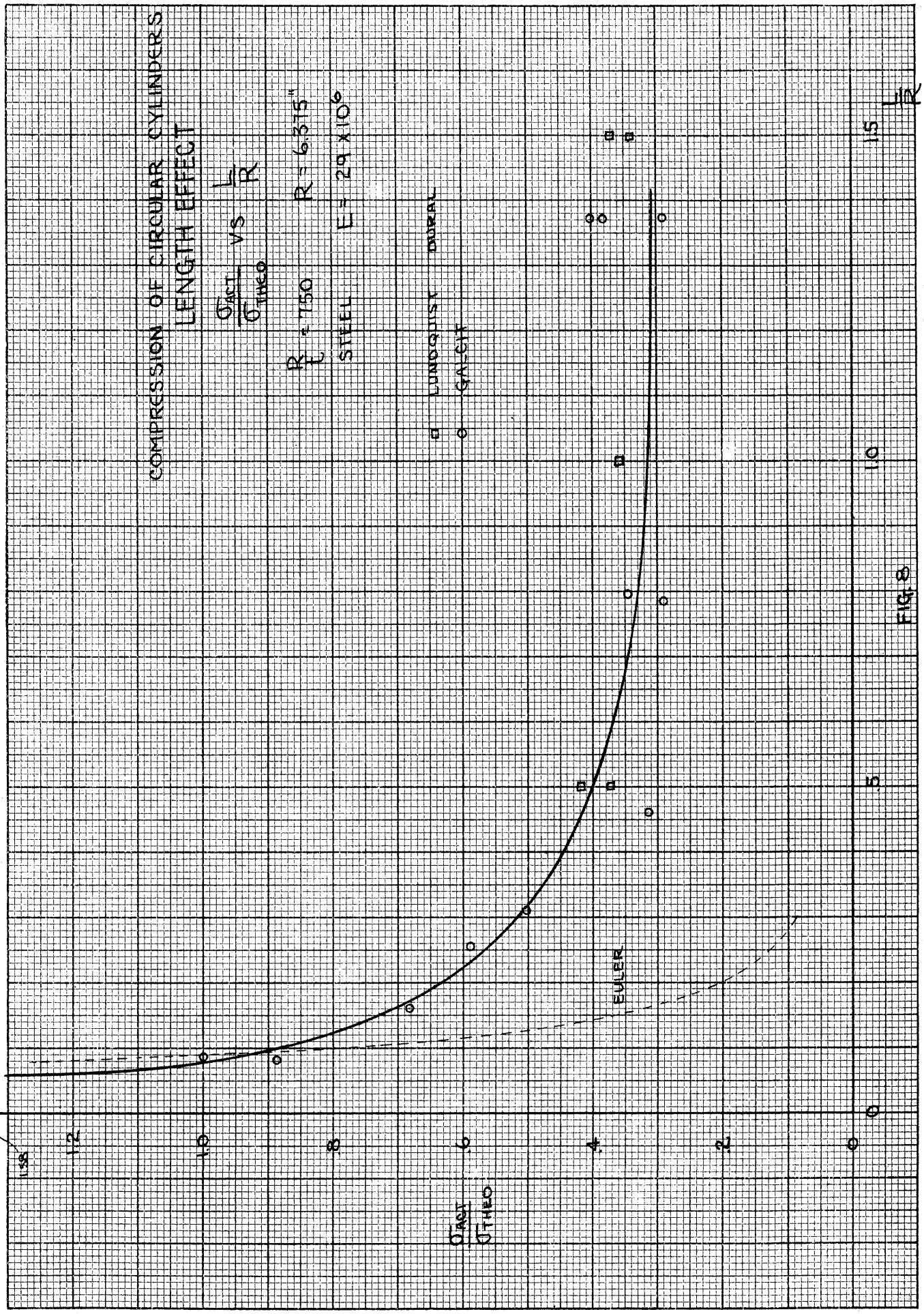
COMPRESSION OF CIRCULAR CYLINDERS
LENGTH EFFECT
$\frac{\sigma_{ACT}}{\sigma_{THEO}}$ VS $\frac{L}{R}$
$\frac{R}{t}$ = 750
R = 6.375"
STEEL E = 29 x 10⁶
LUNDQUIST DORAL
GA-CIT
EULER
$\frac{\sigma_{ACT}}{\sigma_{THEO}}$
$\frac{L}{R}$
1.38
0
2
4
6
8
10
12
15

FIG. 8

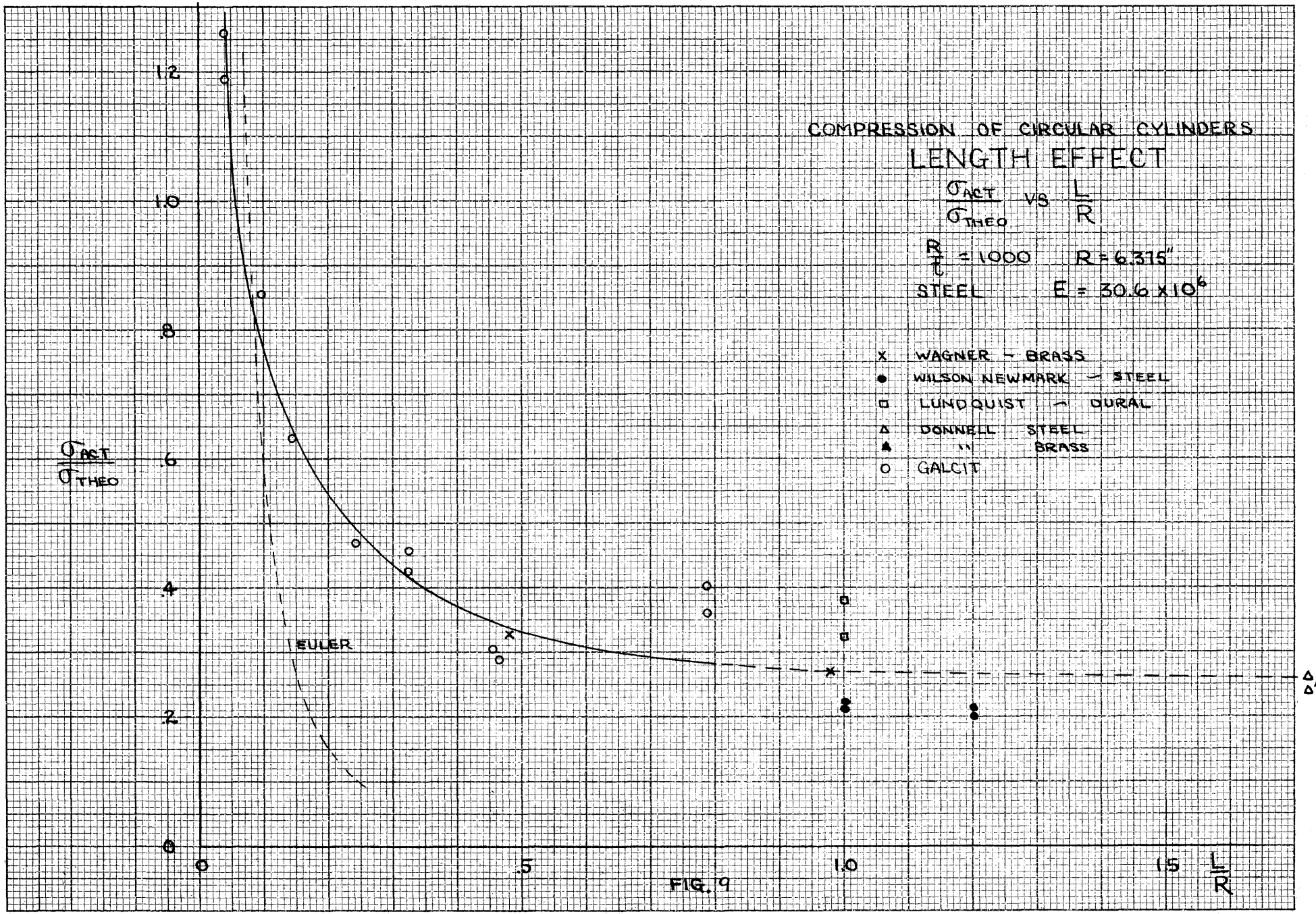
COMPRESSION OF CIRCULAR CYLINDERS
LENGTH EFFECT
$\frac{\sigma_{ACT}}{\sigma_{THEO}}$ VS $\frac{L}{R}$
$\frac{R}{t}$ = 1000 R = 6.315"
STEEL E = 30.6 x 10^6
x WAGNER - BRASS
● WILSON NEWMARK - STEEL
□ LUNDQUIST - DURAL
△ DONNELL STEEL
▲ " BRASS
○ GALCIT
EULER
$\frac{\sigma_{ACT}}{\sigma_{THEO}}$
1.2
1.0
.8
.6
.4
.2
0
0
.5
1.0
1.5
$\frac{L}{R}$
$\frac{L}{R}$=2

FIG. 9

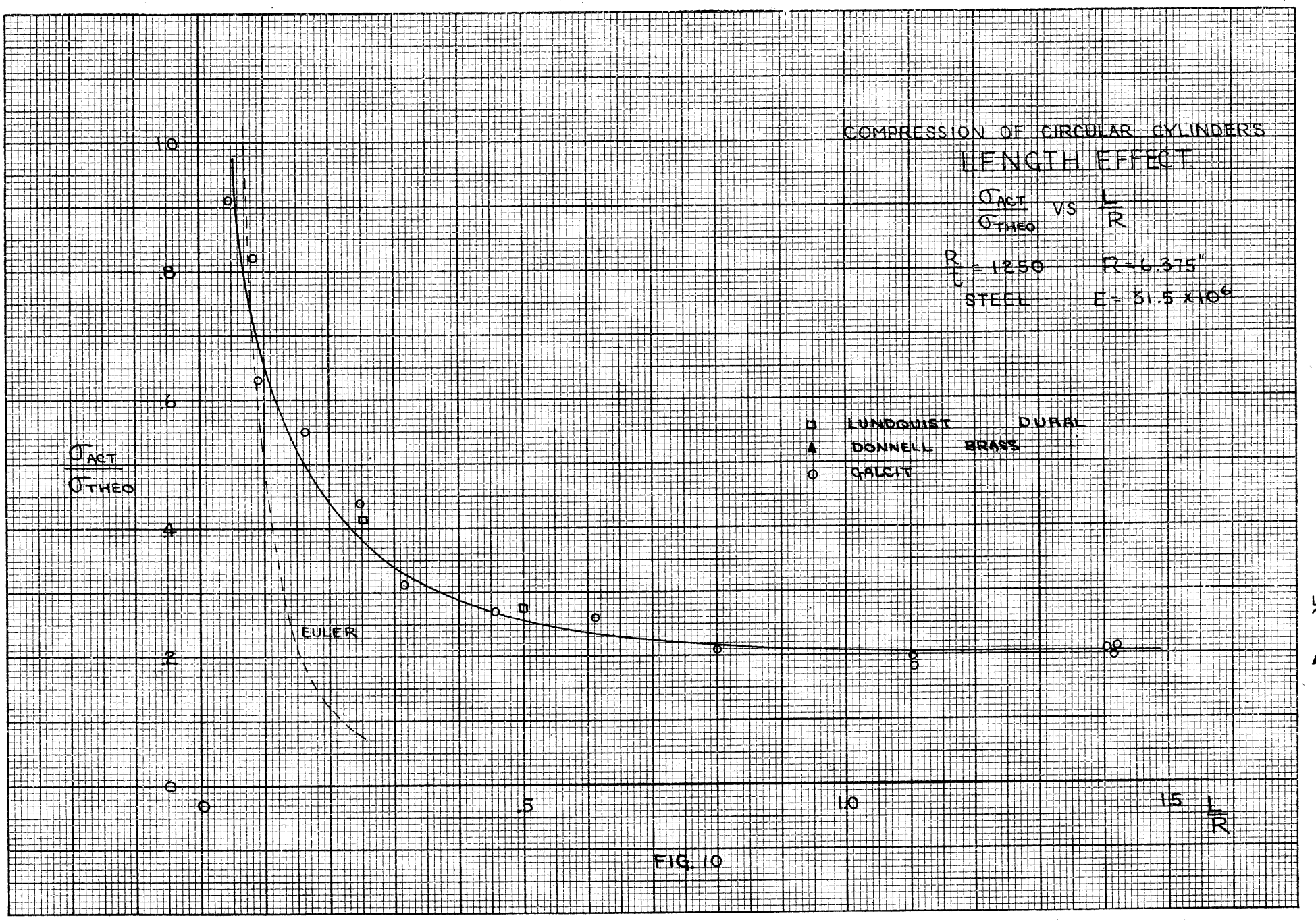
COMPRESSION OF CIRCULAR CYLINDERS
LENGTH EFFECT
$\frac{\sigma_{ACT}}{\sigma_{THEO}}$ VS $\frac{L}{R}$
$\frac{R}{t}$ = 1250 R = 6.375"
STEEL E = 31.5 x 10⁶
LUNDQUIST DURAL
DONNELL BRASS
GALCIT
EULER
$\frac{\sigma_{ACT}}{\sigma_{THEO}}$
10
8
6
4
2
0
.5
1.0
1.5
$\frac{L}{R}$
$\frac{L}{R}$=2

FIG. 10

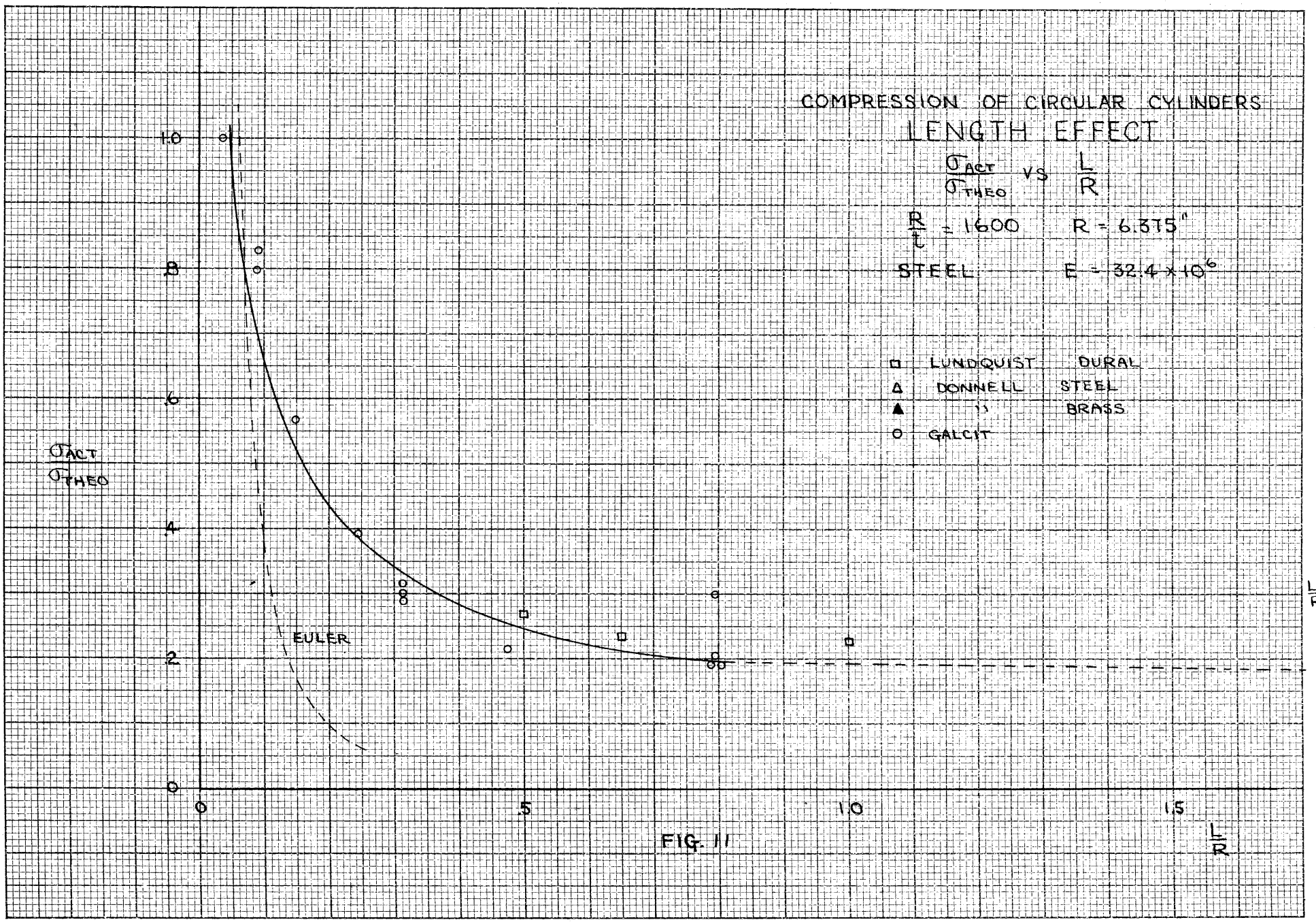
COMPRESSION OF CIRCULAR CYLINDERS
LENGTH EFFECT
$\frac{\sigma_{ACT}}{\sigma_{THEO}}$ VS $\frac{L}{R}$
$\frac{R}{t}$ = 1600 R = 6.375"
STEEL E = 32.4 x 10^6
LUNDQUIST DURAL
DONNELL STEEL
" BRASS
GALCIT
$\frac{\sigma_{ACT}}{\sigma_{THEO}}$
EULER
1.0
8
6
4
2
0
0
.5
1.0
1.5
$\frac{L}{R}$
$\frac{L}{R}$ = 2

FIG. 11

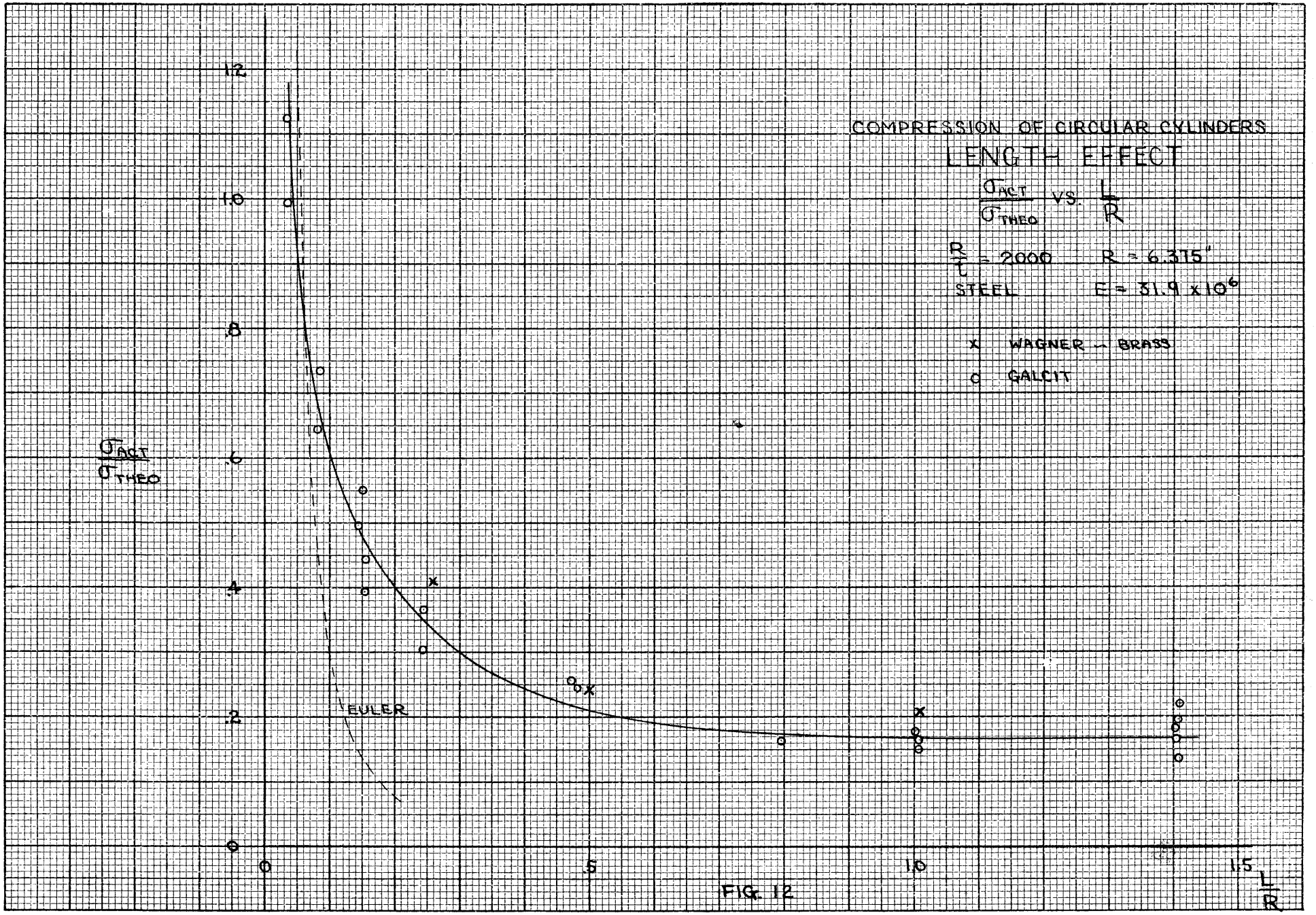
COMPRESSION OF CIRCULAR CYLINDERS
LENGTH EFFECT
$\frac{\sigma_{ACT}}{\sigma_{THEO}}$ VS. $\frac{L}{R}$
$R_u$ = 2000 R = 6.375"
STEEL E = 31.9 x 10⁶
x WAGNER -- BRASS
o GALCIT
$\frac{\sigma_{ACT}}{\sigma_{THEO}}$
1.2
1.0
.8
.6
.4
.2
0
EULER
0
5
10
15
$\frac{L}{R}$

FIG. 12

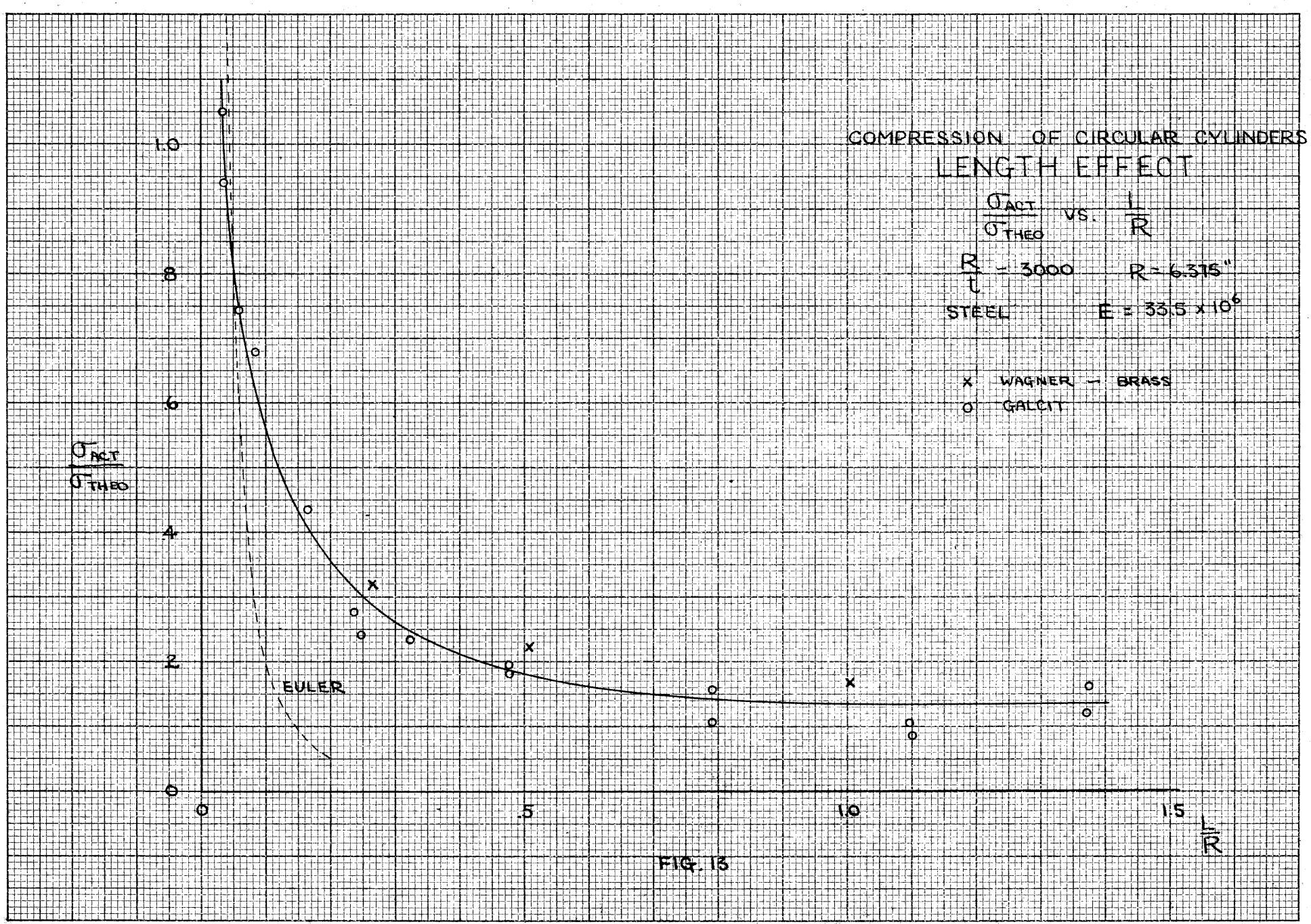
COMPRESSION OF CIRCULAR CYLINDERS
LENGTH EFFECT
σACT / σTHEO VS. L/R
R/t = 3000
R = 6.315"
STEEL
E = 33.5 x 10^6
x WAGNER – BRASS
o GALCIT
σACT / σTHEO
1.0
.8
.6
.4
.2
0
EULER
0
.5
1.0
1.5
L/R

FIG. 13

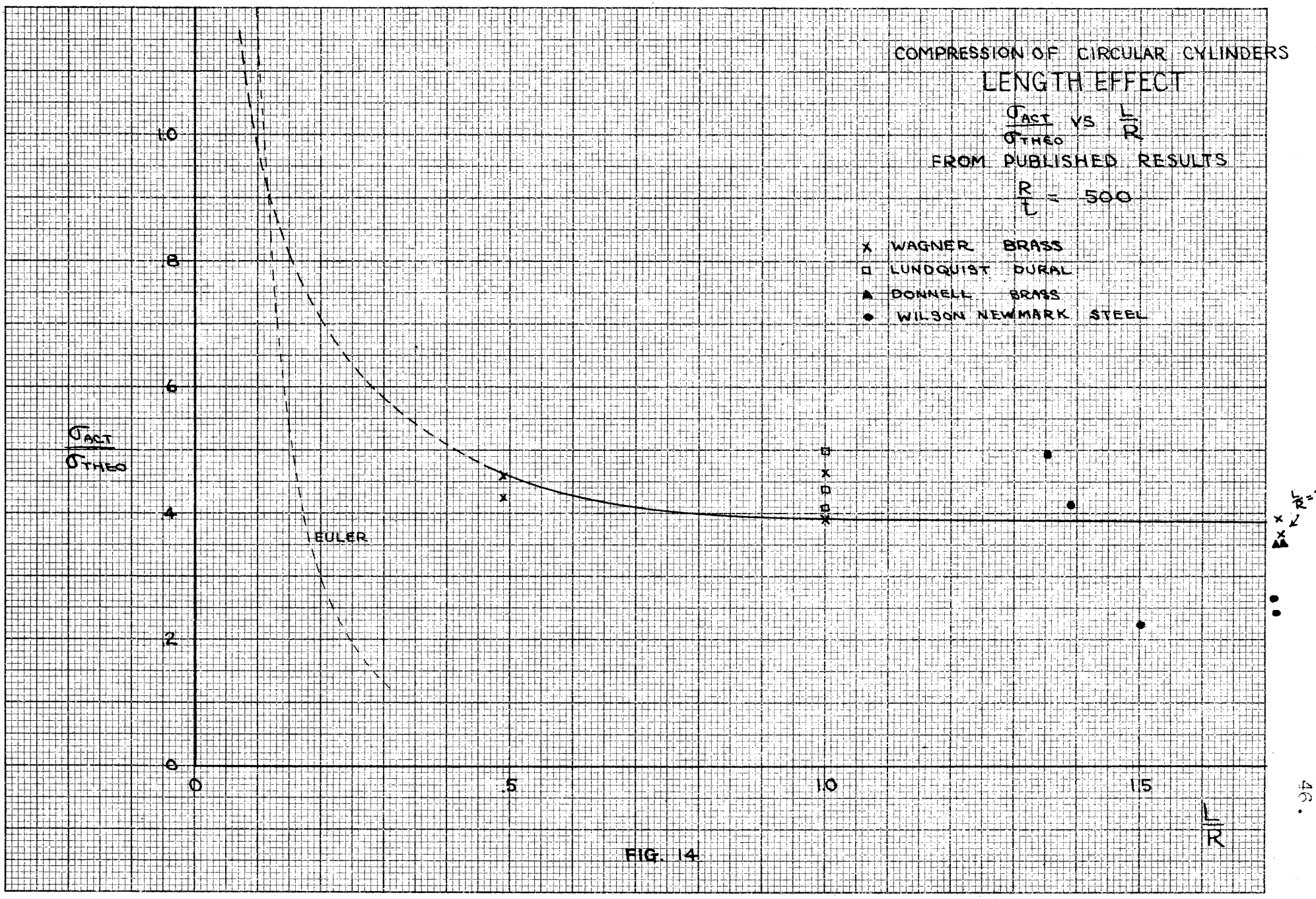
COMPRESSION OF CIRCULAR CYLINDERS
LENGTH EFFECT
$\frac{\sigma_{ACT}}{\sigma_{THEO}}$ VS $\frac{L}{R}$
FROM PUBLISHED RESULTS
$\frac{R}{t}$ = 500
x WAGNER BRASS
□ LUNDQUIST DURAL
▲ DONNELL BRASS
● WILSON NEWMARK STEEL
$\frac{\sigma_{ACT}}{\sigma_{THEO}}$
EULER
1.0
.8
.6
.4
.2
0
0
.5
1.0
1.5
$\frac{L}{R}$
$\frac{L}{R}$=2

FIG. 14

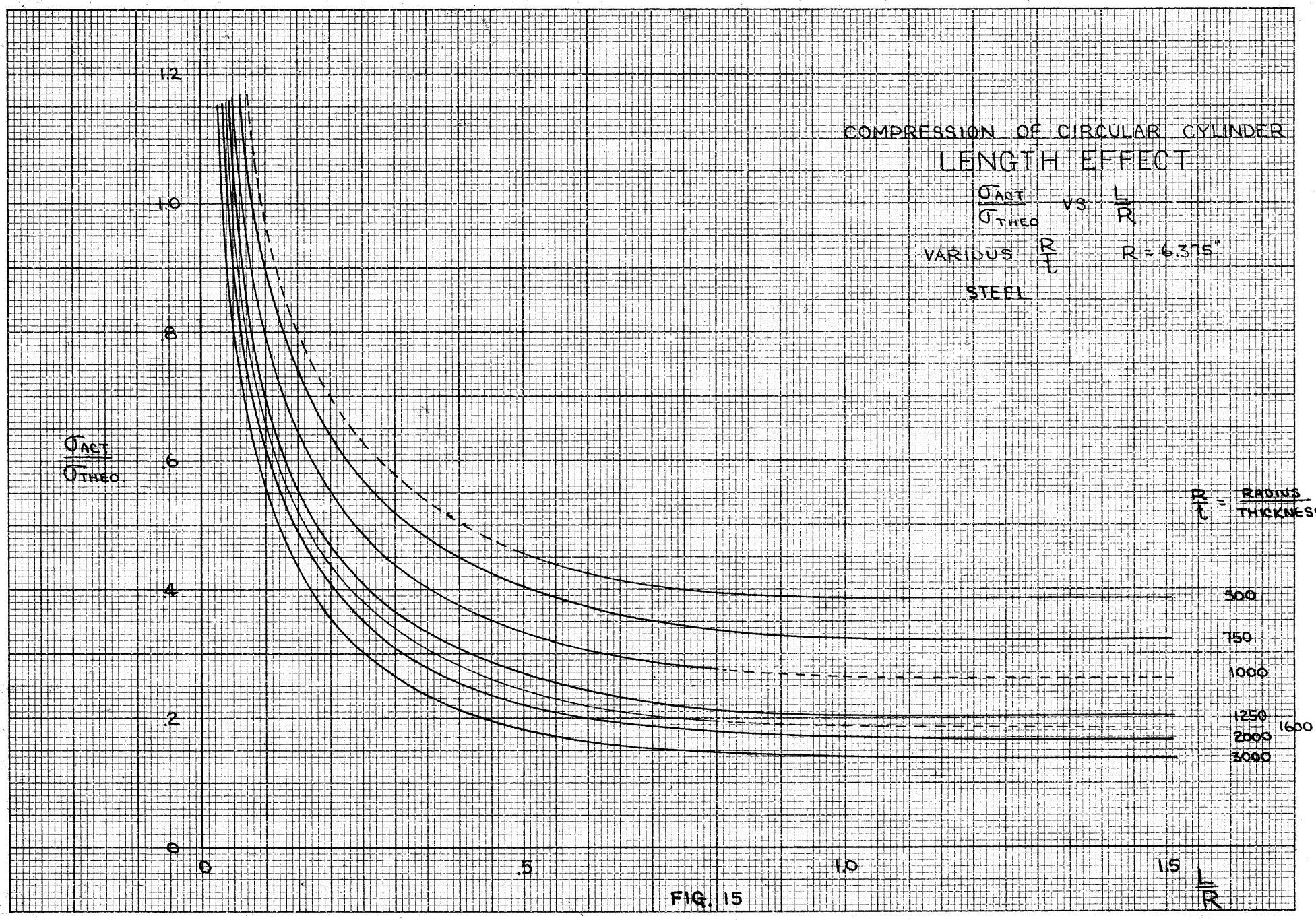
COMPRESSION OF CIRCULAR CYLINDER
LENGTH EFFECT
σACT / σTHEO VS L/R
VARIOUS R/t R = 6.375"
STEEL
σACT / σTHEO
R/t = RADIUS / THICKNESS
500
750
1000
1250
1600
2000
3000
1.2
1.0
.8
.6
.4
.2
0
0
.5
1.0
1.5
L/R

FIG. 15

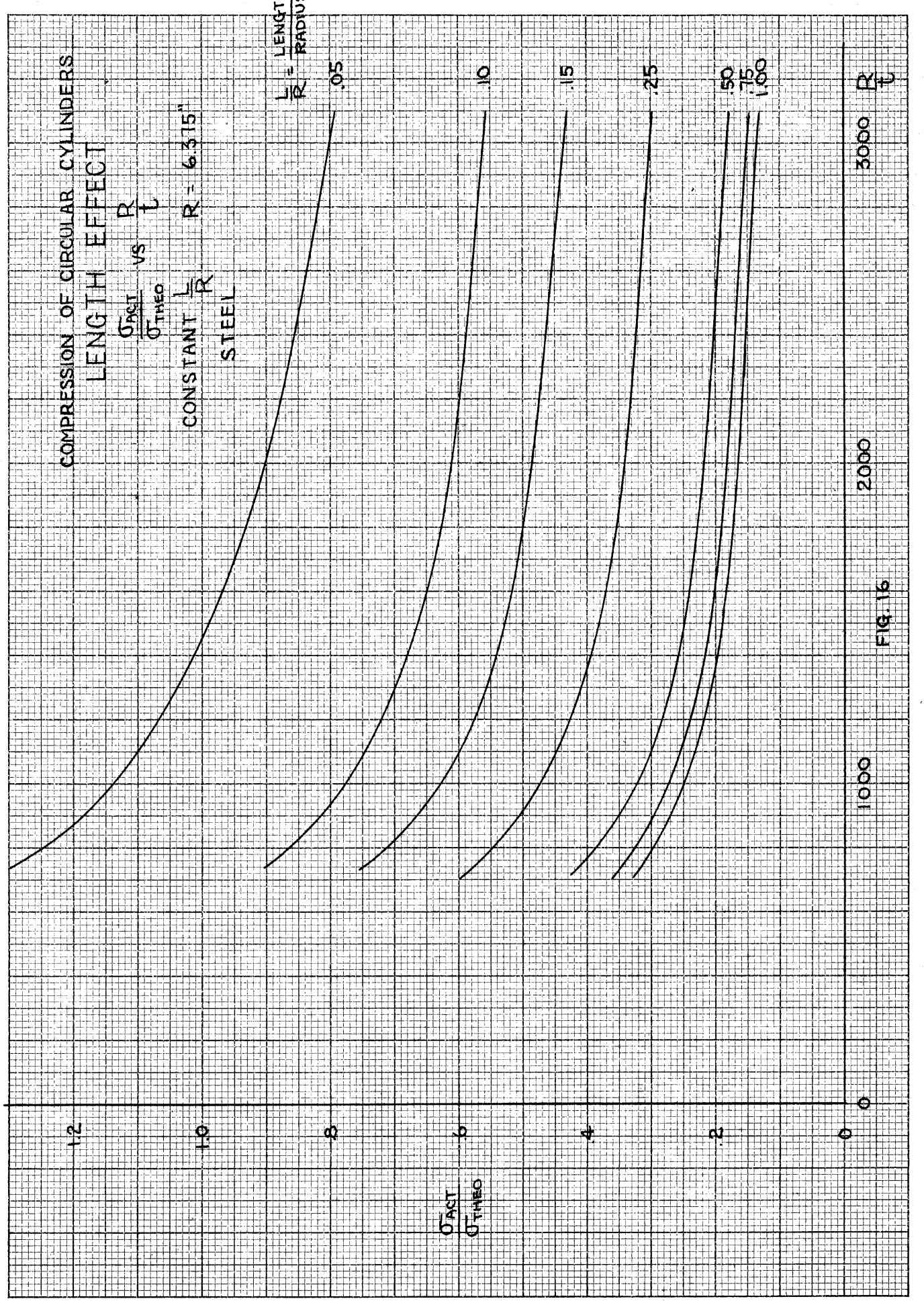
COMPRESSION OF CIRCULAR CYLINDERS
LENGTH EFFECT
$\frac{\sigma_{ACT}}{\sigma_{THEO}}$ VS $\frac{R}{t}$
CONSTANT $\frac{L}{R}$ R = 6.375"
STEEL
$\frac{L}{R}$ = LENGTH / RADIUS
.05
.10
.15
.25
.50
.75
1.00
$\frac{\sigma_{ACT}}{\sigma_{THEO}}$
1.2
1.0
.8
.6
.4
.2
0
0
1000
2000
3000
$\frac{R}{t}$

FIG. 16

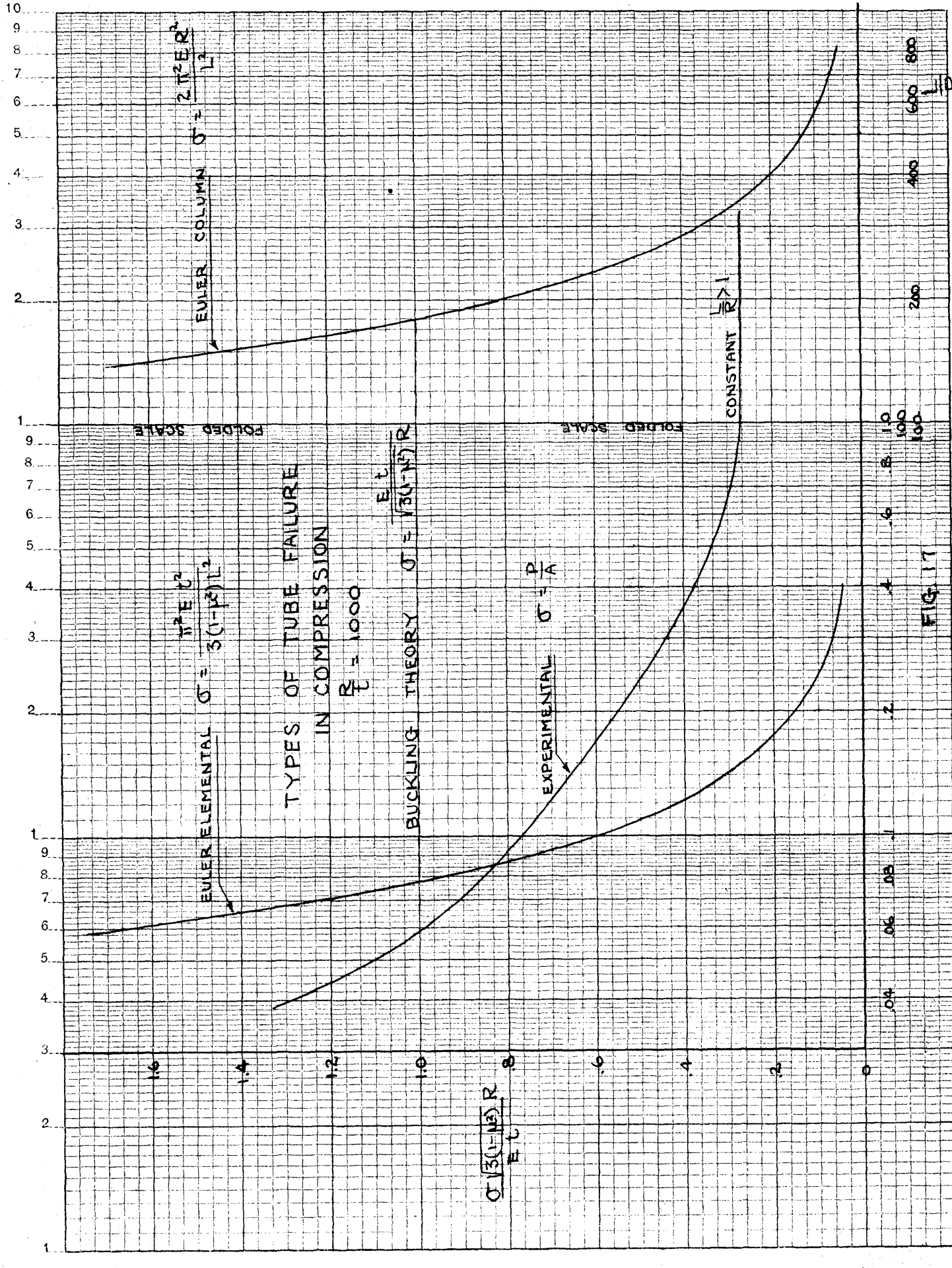
TYPES OF TUBE FAILURE
IN COMPRESSION
$\frac{R}{t}$ = 1000
EULER COLUMN $\sigma = \frac{2\pi^2 E R^2}{L^2}$
EULER ELEMENTAL $\sigma = \frac{\pi^2 E t^2}{3(1-\mu^2)L^2}$
BUCKLING THEORY $\sigma = \frac{E t^2}{\sqrt{3(1-\mu^2)}R}$
EXPERIMENTAL $\sigma = \frac{P}{A}$
CONSTANT $\frac{L}{R} > 1$
FOLDED SCALE
FOLDED SCALE
$\sigma \sqrt{\frac{3(1-\mu^2)}{E}} \frac{R}{t}$
$\frac{L}{R}$
FIG. 17

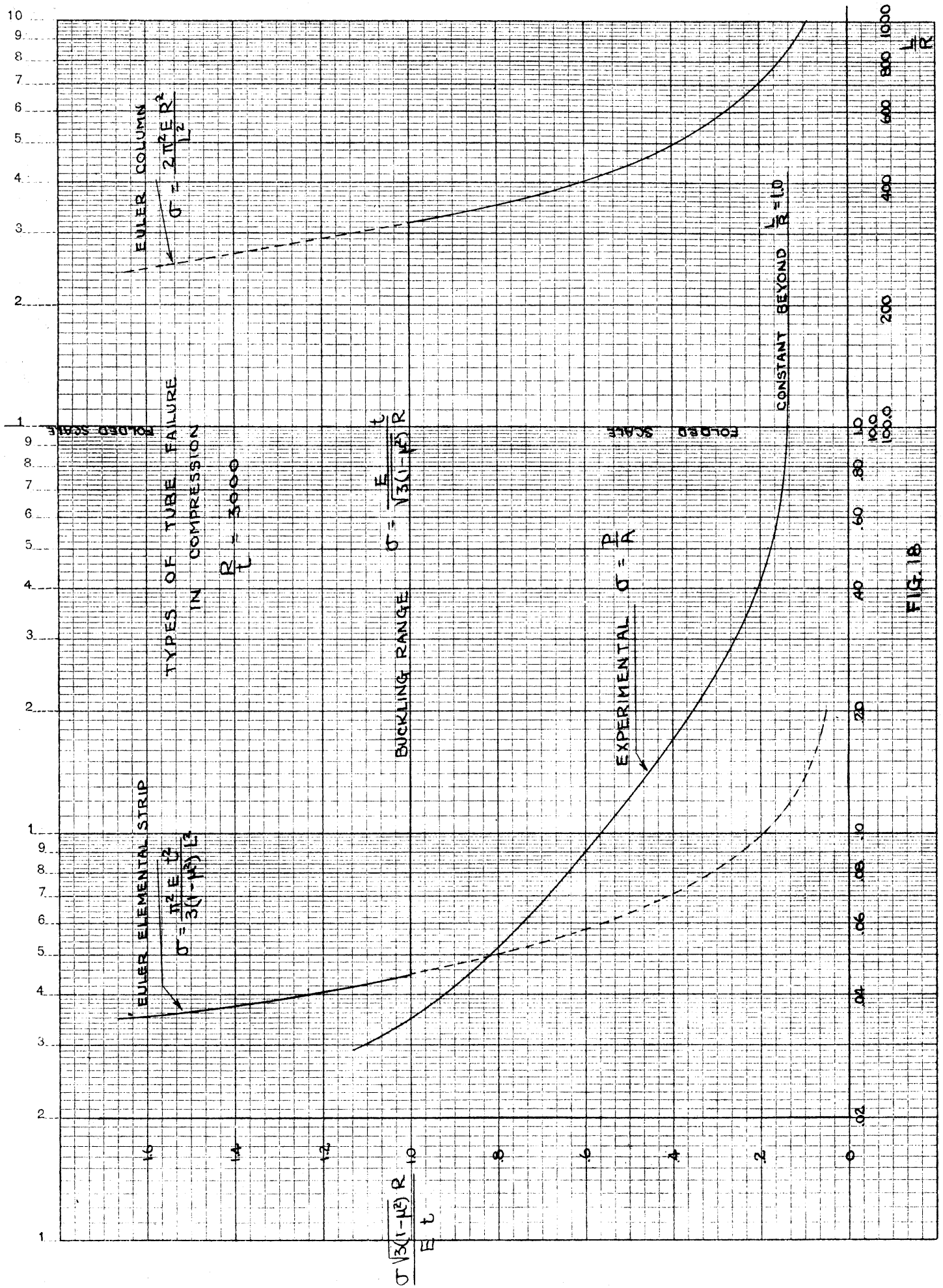
EULER COLUMN
$\sigma = \frac{2\pi^2 E R^2}{L^2}$
TYPES OF TUBE FAILURE IN COMPRESSION
$\frac{R}{t} = 3000$
$\sigma = \frac{E}{\sqrt{3(1-\mu^2)}} \frac{t}{R}$
BUCKLING RANGE
FOLDED SCALE
CONSTANT BEYOND $\frac{L}{R} = 1.0$
EXPERIMENTAL $\sigma = \frac{P}{A}$
EULER ELEMENTAL STRIP
$\sigma = \frac{\pi^2 E t^2}{3(1-\mu^2) L^2}$
$\frac{\sigma \sqrt{3(1-\mu^2)}}{E} \frac{R}{t}$
$\frac{L}{R}$

FIG. 18

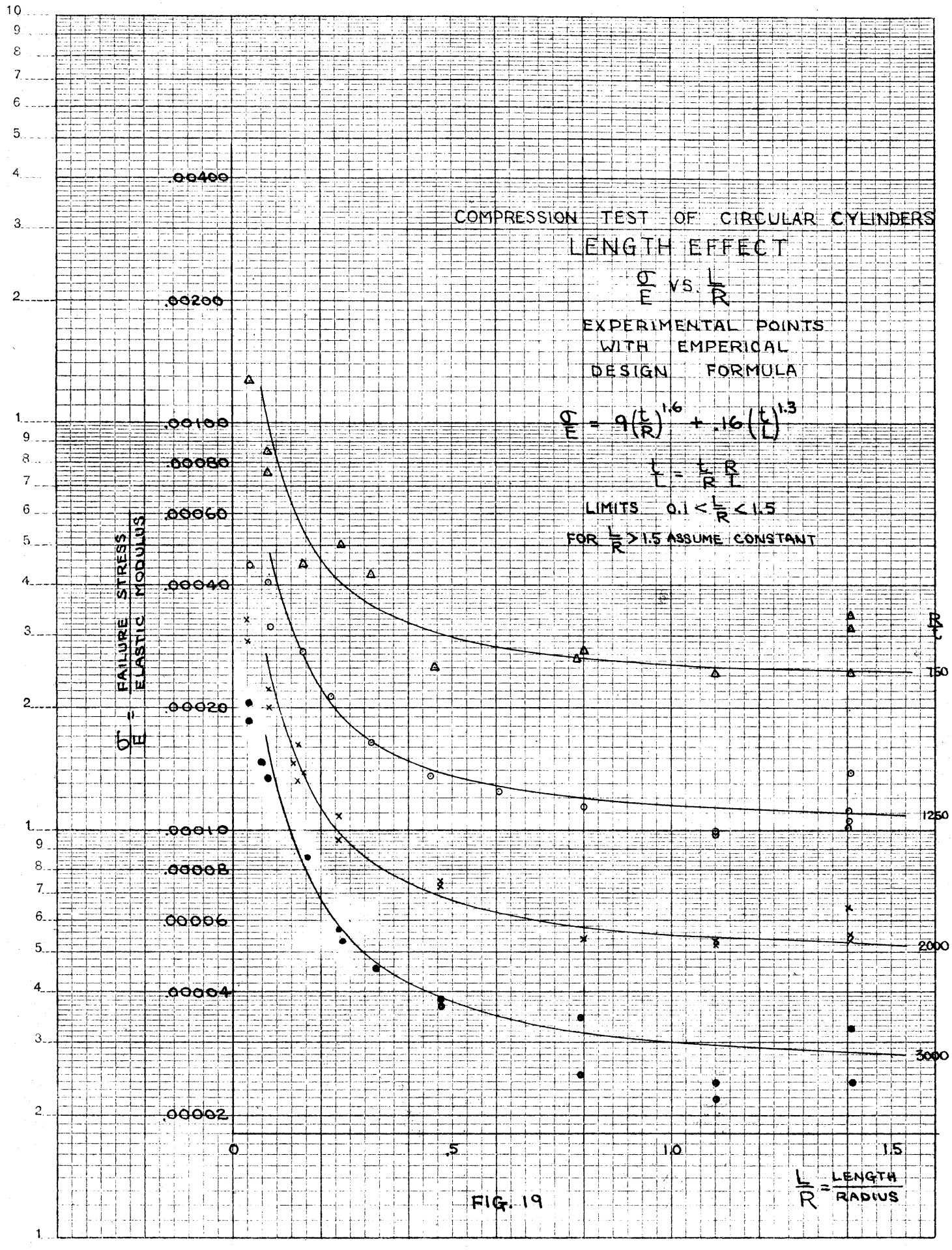
COMPRESSION TEST OF CIRCULAR CYLINDERS
LENGTH EFFECT
σ/E VS. L/R
EXPERIMENTAL POINTS WITH EMPERICAL DESIGN FORMULA
σ/E = 9(t/R)^1.6 + .16(t/L)^1.3
t/L = t/R · R/L
LIMITS 0.1 < L/R < 1.5
FOR L/R > 1.5 ASSUME CONSTANT
σ/E = FAILURE STRESS / ELASTIC MODULUS
.00400
.00200
.00100
.00080
.00060
.00040
.00020
.00010
.00008
.00006
.00004
.00002
R/t
150
1250
2000
3000
0
.5
1.0
1.5
L/R = LENGTH / RADIUS

FIG. 19

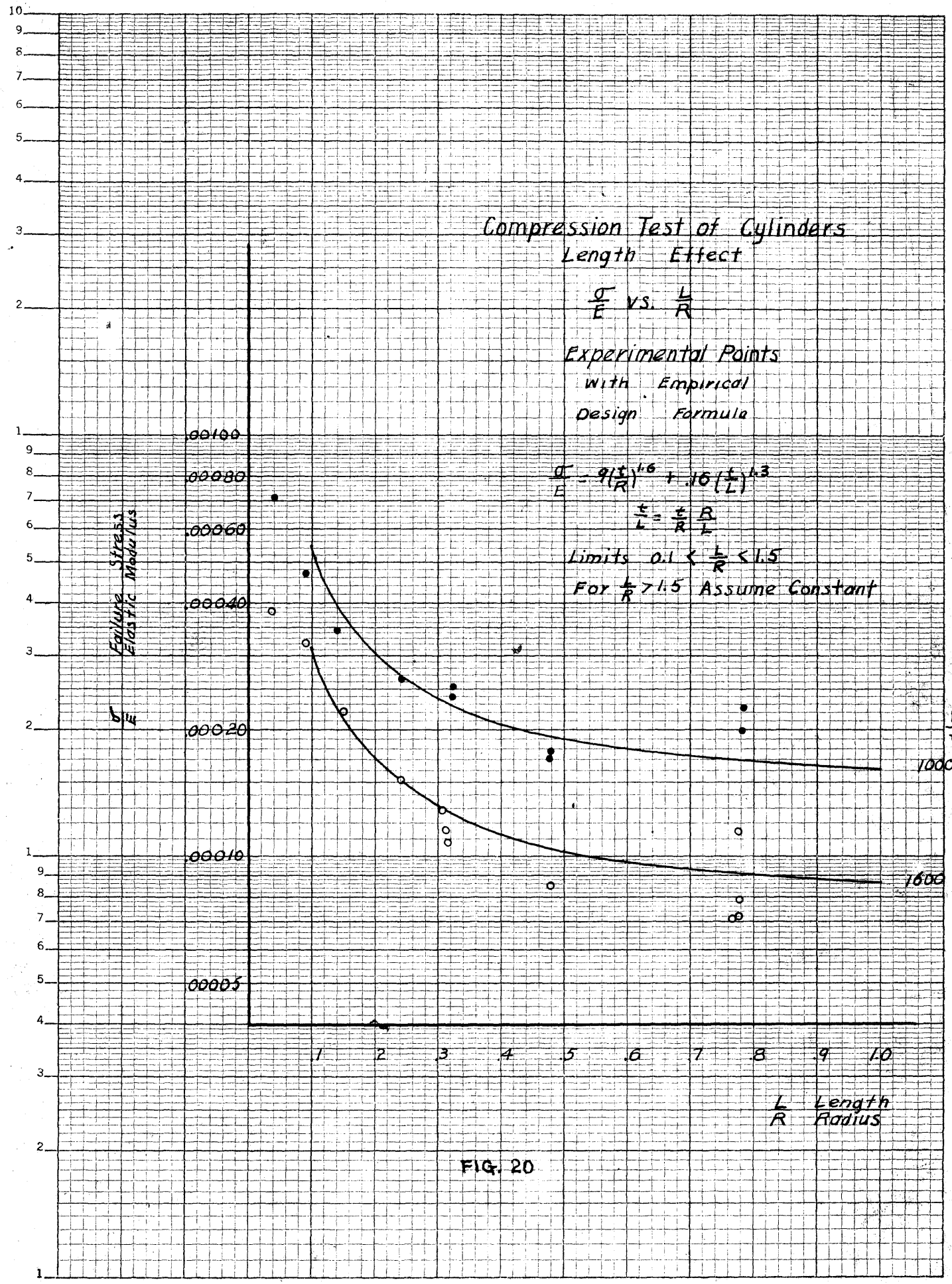
Compression Test of Cylinders
Length Effect
$\frac{\sigma}{E}$ vs. $\frac{L}{R}$
Experimental Points
With Empirical
Design Formula
$\frac{\sigma}{E} = 9\left(\frac{t}{R}\right)^{1.6} + .16\left(\frac{t}{L}\right)^{1.3}$
$\frac{t}{L} = \frac{t}{R}\frac{R}{L}$
Limits $0.1 < \frac{L}{R} < 1.5$
For $\frac{L}{R} > 1.5$ Assume Constant
Failure Stress / Elastic Modulus
.00100
.00080
.00060
.00040
.00020
.00010
.00005
1
2
3
4
5
6
7
8
9
10
$\frac{R}{t}$
1000
1600
$\frac{L}{R}$ Length / Radius

FIG. 20

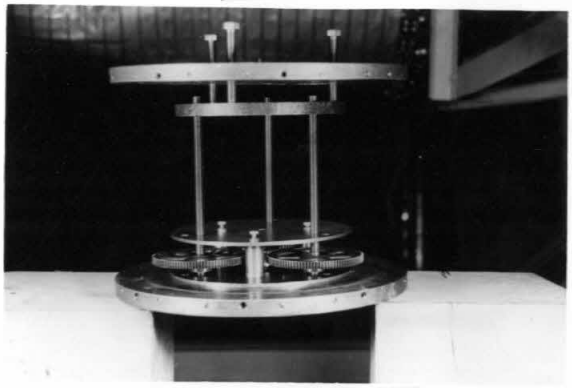

Fig. 21
Head Lowering
Mechanism.

FIG. 50

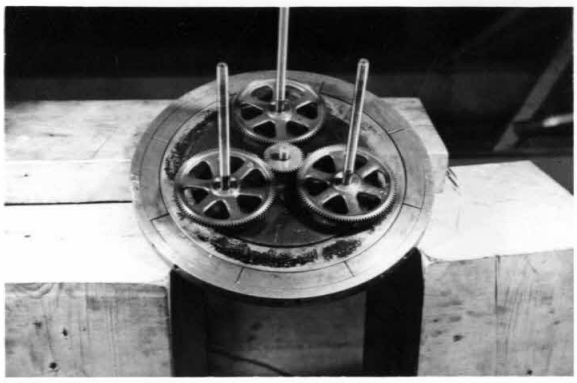

Fig. 22
Gear System

FIG. 51

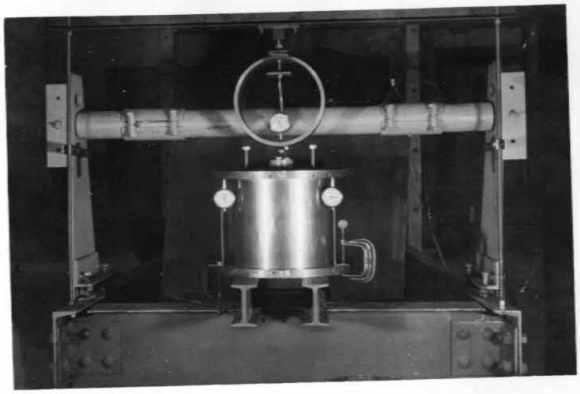

Fig.23
Loading
apparatus

FIG. 52

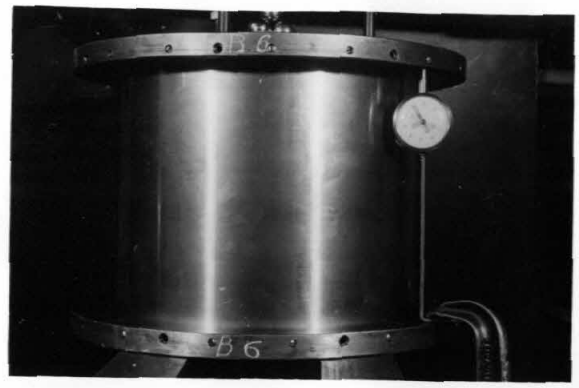


Fig. 24
No Load


Fig. 25
First Buckle

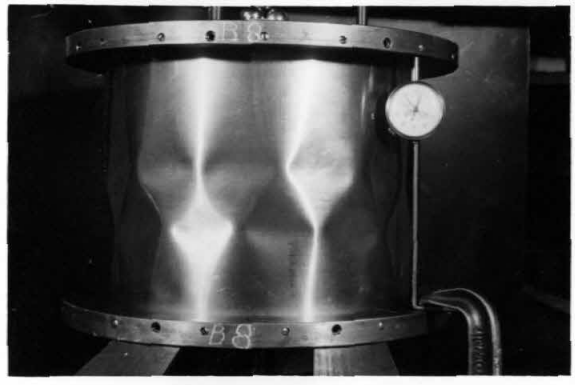


Fig. 26
Failure


FIG. 53

Fig.27

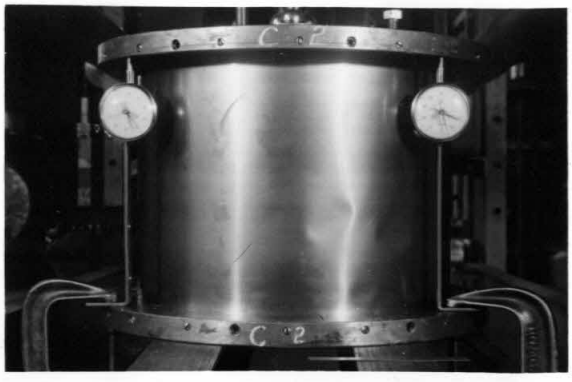


FIG. 54

Fig. 28

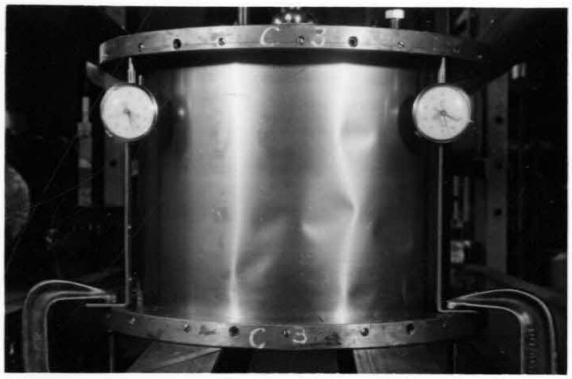


FIG. 55

Fig. 29

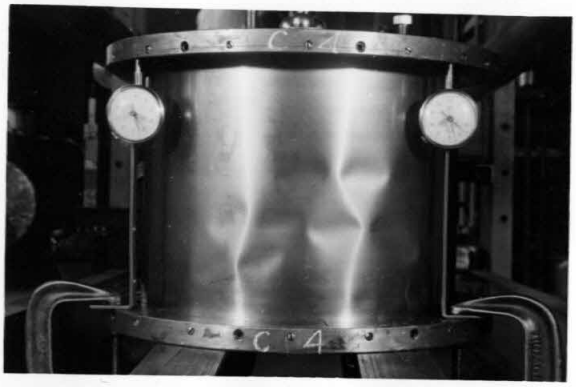


Fig. 30 FIG. 56

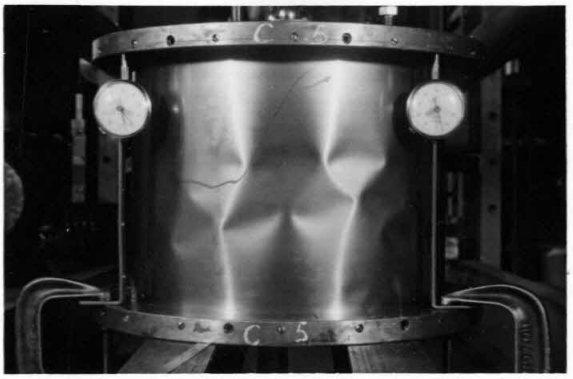


Fig. 31 FIG. 57

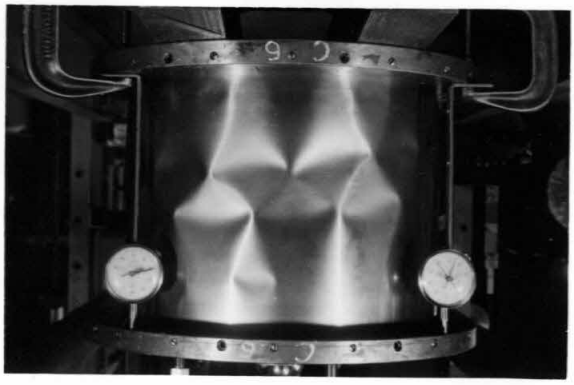


Fig. 32 FIG. 58

upside down

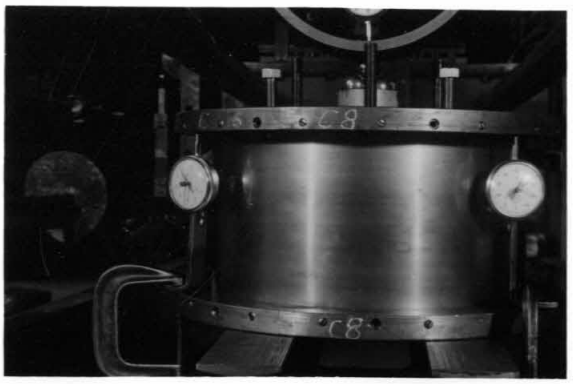


Fig. 33 FIG. 59

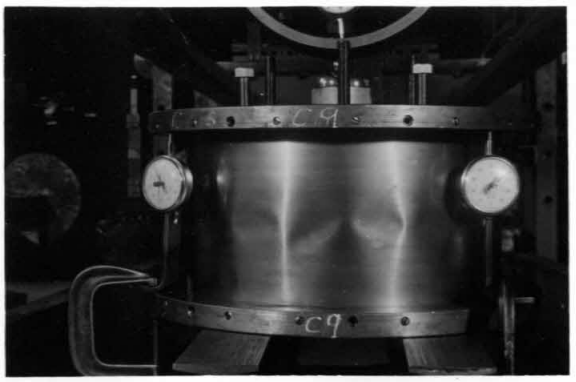


Fig. 34 FIG. 60

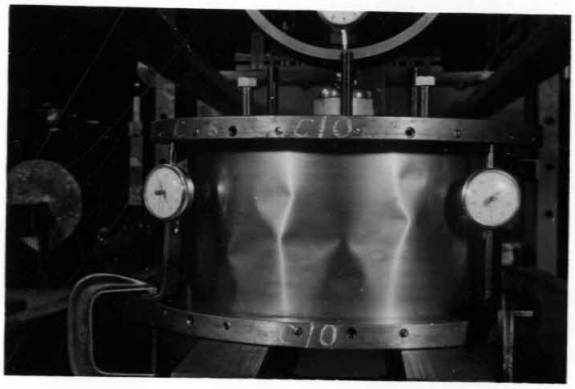


Fig. 35 FIG. 61

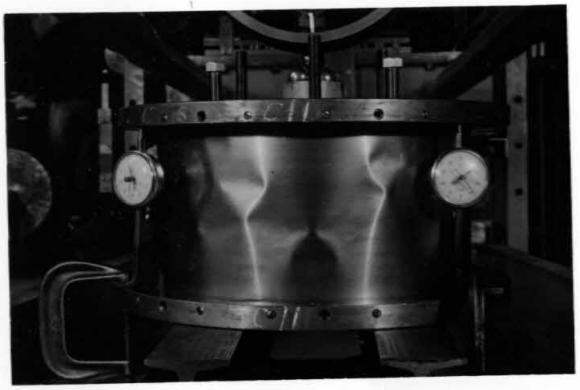


Fig. 36 FIG. 62

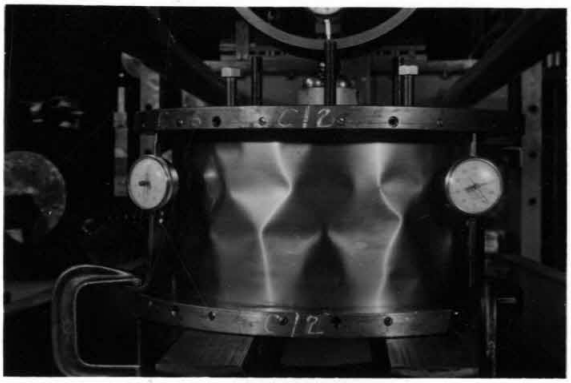


Fig. 37 FIG. 63

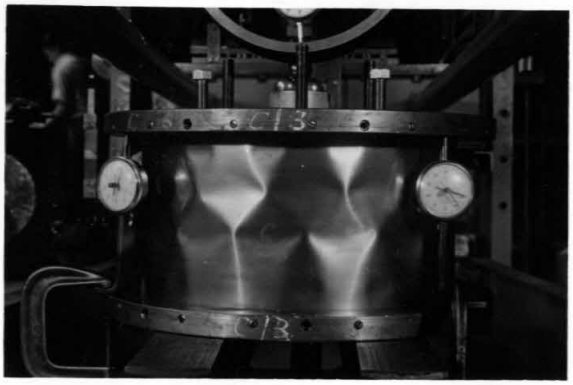


Fig. 38 FIG. 64

Z-5
(for History)

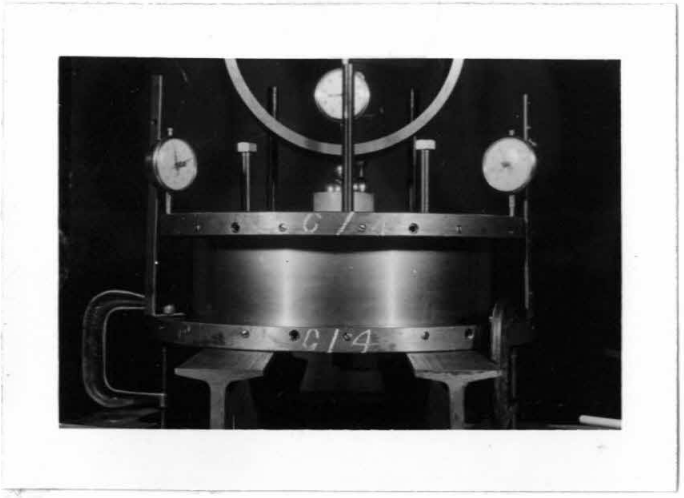


Fig. 39

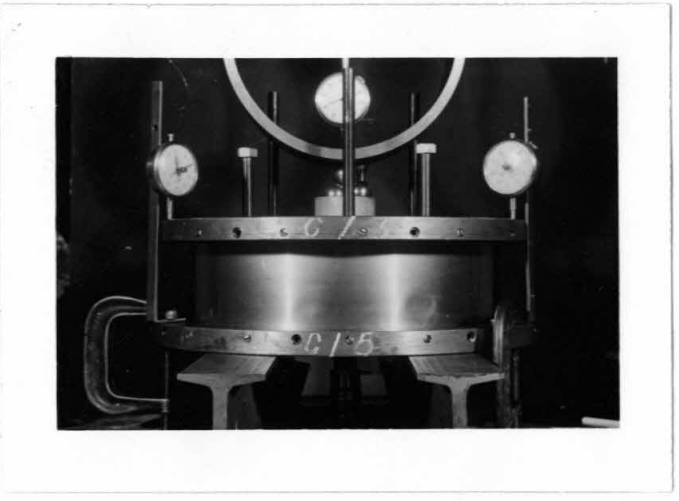


Fig. 40

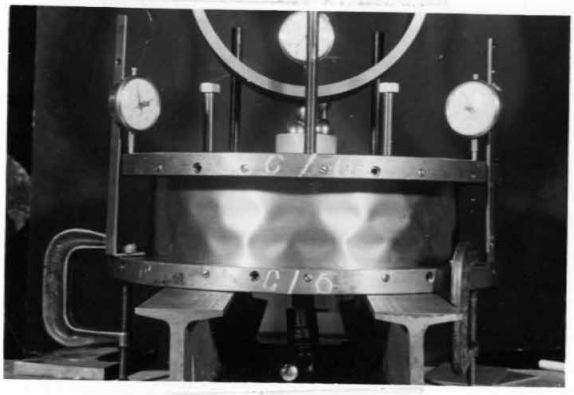


Fig. 41

FIG. 49

REFERENCES

1. Timoshenko, S.: Theory of Elastic Stability
Mc Graw Hill Book Company, Inc. New York & London
Chap. VIII & IX 1936

2. Southwell, R. V.: On the General Theory of Elastic Stability
Phil. Trans. Roy. Soc. (London)
Vol. 213, series A. 1914

3. Dean W. R.: On the Theory of Elastic Stability
Proc. Roy. Soc. (London)
Vol. 107, series A pp. 734-759

4. Robertson, Andrew: The Strength of Tubular Struts
R. & M. 1185 British A. R. C.
Vol. II 1929

5. Wilson, W. And Newmark, N.: The Strength of Thin Cylindrical Shells as Columns
Bull. No. 255 Eng. Exp. Sta. Univ. Ill. 1933

6. Sanden, K. and Tolke, F.: Uber Stabilitats Probleme Dunner, Kreiszylindrischer Schalen
Ingenieur-Archiv Band 3 Heft 1 1932
pp. 24-66

7. Flugge, W.: Die Stabilitat der Kreiszylinderschale
Ingenieur-Archiv Band 3 Heft 5 1932
pp. 463-506

8. Donnell, L.: A New Theory for the Buckling of Thin Cylinders Under Axial Compression and Bending
Trans. A. S. M. E. Aero. Engin. Nov. 1934
(see also GALCIT publication No. 50)

9. Lundquist, E. : Strength Test of Thin-walled Duraliemin Cylinders in Compression
NACA, TR. 473, 1938

10. Ballerstedt and Wagner, H.: Versuch über die Festigkeit Dünner Unversteifter Zylinder
Luftfahrt forchung page 306 1936